Dielectric Response at THz Frequencies of Mg Water Complexes Interacting with O_3 Calculated by Density Functional Theory

L. Huang
S.G. Lambrakos

Center for Computational Materials Science
Materials Science and Technology Division

A. Shabaev

George Mason University
Fairfax, Virginia

L. Massa

Hunter College
New York, New York

C. Yapijakis

The Cooper Union
New York, New York

October 24, 2012

REPORT DOCUMENTATION PAGE

Public reporting burden for this collection of information is estimated to average 1 hour per response, including the time for reviewing instructions, searching existing data sources, gathering and maintaining the data needed, and completing and reviewing this collection of information. Send comments regarding this burden estimate or any other aspect of this collection of information, including suggestions for reducing this burden to Department of Defense, Washington Headquarters Services, Directorate for Information Operations and Reports (0704-0188), 1215 Jefferson Davis Highway, Suite 1204, Arlington, VA 22202-4302. Respondents should be aware that notwithstanding any other provision of law, no person shall be subject to any penalty for failing to comply with a collection of information if it does not display a currently valid OMB control number. **PLEASE DO NOT RETURN YOUR FORM TO THE ABOVE ADDRESS.**

1. REPORT DATE (DD-MM-YYYY) 24-10-2012	2. REPORT TYPE NRL Memorandum Report	3. DATES COVERED (From - To) October 1, 2011 – August 1, 2012

4. TITLE AND SUBTITLE Dielectric Response at THz Frequencies of Mg Water Complexes Interacting with O_3 Calculated by Density Functional Theory	5a. CONTRACT NUMBER
	5b. GRANT NUMBER
	5c. PROGRAM ELEMENT NUMBER
6. AUTHOR(S) L. Huang, S.G. Lambrakos, A. Shabaev,[1] L. Massa,[2] and C. Yapijakis[3]	5d. PROJECT NUMBER
	5e. TASK NUMBER
	5f. WORK UNIT NUMBER 63-9564-L-2-5

7. PERFORMING ORGANIZATION NAME(S) AND ADDRESS(ES) Naval Research Laboratory, Code 6394 4555 Overlook Avenue, SW Washington, DC 20375-5320	8. PERFORMING ORGANIZATION REPORT NUMBER NRL/MR/6390--12-9430

9. SPONSORING / MONITORING AGENCY NAME(S) AND ADDRESS(ES) Office of Naval Research One Liberty Center 875 North Randolph Street, Suite 1425 Arlington, VA 22203-1995	10. SPONSOR / MONITOR'S ACRONYM(S) ONR
	11. SPONSOR / MONITOR'S REPORT NUMBER(S)

12. DISTRIBUTION / AVAILABILITY STATEMENT

Approved for public release; distribution is unlimited.

13. SUPPLEMENTARY NOTES

[1]George Mason University, Department of Computation and Data Sciences, Fairfax, VA 22030
[2]Hunter College, City University of New York, New York, NY 10065
[3]Albert Nerkin School of Engineering, The Cooper Union, New York, NY 10003

14. ABSTRACT

The need for better monitoring of water quality and levels of water contamination implies a need for determining the dielectric response properties of water contaminants with respect to electromagnetic wave excitation. In addition to monitoring contaminants, there is an associated need for monitoring chemical processes whose purpose is deactivation or assistance in the removal of water contaminants. Two naturally occurring water contaminants, which are the result of decaying vegetation, are Iron and Manganese, where Iron is in general at much higher concentrations. Correspondingly, a process that is highly effective for assisting filtration of water contaminants, including Iron and Manganese, is the addition in solution of Ozone, i.e., the preozonation process. The present study is based on significant progress in density functional theory (DFT), and associated software technology, which is sufficiently mature for the determination of dielectric response functions, and actually provides complementary information to that obtained from experiment. This point is further demonstrated in this study by calculations of ground state resonance structure associated with water complexes of Mg and the interaction of these complexes with Ozone using DFT. The calculation of ground state resonance structure is for the construction of parameterized dielectric response functions for excitation by electromagnetic waves at frequencies within the THz range. The THz range is associated with ground state resonance structure, in contrast to frequencies that can induce appreciable electronic state transitions. Dielectric functions provide for different types of analyses concerning the dielectric response of water contaminants. In particular, these dielectric response functions provide quantitative initial estimates of spectral response features for subsequent adjustment with respect to additional information such as laboratory measurements and other types of theory-based calculations. With respect to qualitative analysis, these spectra provide for the molecular level interpretation of response structure. The DFT software GAUSSIAN was used for the calculations of ground state resonance structure presented here.

15. SUBJECT TERMS

Density functional theory (DFT)	Dielectric functions	Ground state resonance	Water complexes

16. SECURITY CLASSIFICATION OF:			17. LIMITATION OF ABSTRACT	18. NUMBER OF PAGES	19a. NAME OF RESPONSIBLE PERSON Samuel G. Lambrakos
a. REPORT Unclassified Unlimited	b. ABSTRACT Unclassified Unlimited	c. THIS PAGE Unclassified Unlimited	UU	65	19b. TELEPHONE NUMBER (include area code) (202) 767-2601

Contents

Introduction

The need for better monitoring of water quality and levels of water contamination implies a need for determining the dielectric response properties of water contaminants with respect to electromagnetic wave excitation. In addition to monitoring contaminants, there is an associated need for monitoring chemical processes whose purpose is deactivation or assistance in the removal of water contaminants. Two naturally occurring water contaminants, which are the result of decaying vegetation, are Iron and Manganese, where Iron is in general at much higher concentrations. Correspondingly, a process that is highly effective for assisting filtration of water contaminants, including Iron and Manganese, is the addition in solution of Ozone, i.e., the preozonation process. The present study is based on significant progress in density functional theory (DFT), and associated software technology, which is sufficiently mature for the determination of dielectric response functions, and actually provides complementary information to that obtained from experiment. The calculation of ground state resonance structure is for the construction of parameterized dielectric response functions for excitation by electromagnetic waves at frequencies within the THz range. The THz range is associated with frequencies that are characteristically perturbative to molecular states, and thus represent ground state resonance structure, in contrast to frequencies that can induce appreciable electronic state transitions. Dielectric functions provide for different types of analyses concerning the dielectric response of water contaminants. In particular, these dielectric response functions provide quantitative initial estimates of spectral response features for subsequent adjustment with respect to additional information such as laboratory measurements and other types of theory based calculations. With respect to qualitative analysis, these spectra provide for the molecular level interpretation of response structure. The DFT software GAUSSIAN was used for the calculations of ground state resonance structure presented here.

Typically, the dielectric response properties for electromagnetic wave excitation at THz frequencies, as well as at other frequencies, are determined by means of experimental measurements. The present study is based on significant progress in density functional theory (DFT), and associated software technology, which is sufficiently mature for the determination of dielectric response functions, and actually provides complementary information to that obtained from experiment. In particular, these dielectric response functions provide quantitative initial estimates of spectral response features that can be adjusted with respect to additional information such as laboratory measurements and other types of theory based calculations, as well as providing for the molecular level interpretation of response structure.

Density functional theory has been successfully used to investigate the vibrational spectra of energetic materials in the form of single molecules and molecular crystals [1-7]. These calculations provide detection signatures for various forms of materials, which can be encountered in various detection scenarios [8,9]. The isolated-molecule simulation results help to identify intramolecular vibrational modes in the absorption spectra of various materials. A series of studies have focused on the general concept of constructing dielectric response functions using DFT for the purpose of quantitative simulation of explosives detection scenarios [9,10,11]. As emphasized in these studies, the construction of permittivity functions using DFT calculations, defines a general approach where dielectric response is estimated within the bounds of relatively well-defined adjustable parameters. Following this approach, permittivity functions are constructed using DFT calculated absorption spectra under the condition that the calculated

resonance locations are fixed, while resonance widths and number densities are assumed adjustable with respect to additional information such as experimentally observed spectra or more advanced theory. It is significant to note that, with respect to practical application, water complexes represent a separate regime for using DFT calculations for construction of dielectric response functions.

A significant aspect of using response spectra calculated by density functional theory, DFT, for the direct construction of dielectric response functions is that it adopts the perspective of computational physics, according to which a numerical simulation represents another source of "experimental" data. This perspective is significant in that a general procedure may be developed for construction of dielectric response functions using DFT calculations as a quantitative initial estimate of spectral response features for subsequent adjustment with respect to additional information such as experimental measurements and other types of theory based calculations. That is to say, for the purpose of simulating many electromagnetic response characteristics of materials, DFT is sufficiently mature for the purpose of generating data complementing, as well as superseding, experimental measurements.

In the case of THz excitation of materials, the procedure of using response spectra calculated using DFT, which is associated with ground state resonance structure, for the direct construction of permittivity functions is well posed owing to the physical characteristic of THz excitation. In particular, it is important to note that the procedure for constructing a permittivity function using response spectra calculated using DFT is physically consistent with the characteristically linear response associated with THz excitation of molecules. Accordingly, one observes a correlation between the advantages of using THz excitation for detection of explosives (and ambient materials) and those for its numerical simulation based on DFT. Specifically, THz excitation is associated with frequencies that are characteristically perturbative to molecular states, in contrast to frequencies that can induce appreciable electronic state transitions. THz excitation does not appreciably induce electronic transitions. Moreover, in the linear (low-intensity) regime, THz excitation can be treated by means of perturbation theory. Of course, the practical aspect of the perturbative character of THz excitation for detection is that detection methodologies can be developed which do not damage materials under examination. The perturbative character of THz excitation with respect to molecular states has significant implications with respect to its numerical simulation based on DFT. It follows then that, owing to the perturbative character of THz excitation, which is characteristically linear, one is able to make a direct association between local oscillations about ground-state minima of a given molecule and THz excitation spectra.

Construction of permittivity functions according to the best fit of available data for a given material corresponding to many different types of experimental measurements has been typically the dominant approach. This approach is extended by using DFT calculations of electromagnetic response as data for construction of permittivity functions. The inclusion of this type of information is significant for accessing what spectral response features at the molecular level are actually detectable with respect to a given set of detection parameters. Accordingly, permittivity functions having been constructed using DFT calculations provide a quantitative correlation between macroscopic material response and molecular structure. Within this context it is not important that the permittivity function be quantitatively accurate for the purpose of being adopted as input for system simulation. Rather, it is important that the permittivity function be qualitatively accurate in terms of specific dielectric response features for the purpose of sensitivity analysis, which is relevant for the assessment of absolute detectability of different

types of molecular structure with respect to a given set of detection parameters. That is to say, permittivity functions that have been determined using DFT can provide a mechanistic interpretation of material response to electromagnetic excitation that could establish the applicability of a given detection methodology for detection of specific molecular characteristics. Within the context of practical application, permittivity functions having been constructed according to the best fit of available data would be "correlated" with those obtained using DFT for proper interpretation of permittivity-function features. Subsequent to establishment of good correlation between DFT and experiment, DFT calculations can be adopted as constraints for the purpose of constructing permittivity functions, whose features are consistent with molecular level response, for adjustment relative to specific sets of either experimental data or additional molecular level information. In what follows, calculations are presented of ground state resonance structure associated with water complexes of Fe and the interaction of these complexes with Ozone, which is for the construction of parameterized dielectric response functions for excitation by electromagnetic waves at compatible frequencies. For this purpose the DFT software GAUSSIAN09 (G09) was adopted [12].

The organization of the subject areas presented here are as follows. First, a brief example is presented of the significance of Iron and Manganese concentrations in water and of their interaction with Ozone. Second, a brief description is presented of vibrational analysis using DFT for the calculation of absorption spectra and of the construction of permittivity functions using DFT calculated spectra. This includes a general review of the formal structure of permittivity functions in terms of analytic function representations. An understanding of the formal structure of permittivity functions in terms of both physical consistency and causality is important for post-processing of DFT calculations for the purpose of constructing permittivity functions. Third, information concerning the ground state resonance structure of Mg water complexes and of their interaction with Ozone, which is obtained using DFT, is presented. This information consists of the ground state molecular geometries and response spectra for different types of Mg water complexes, with and without the presence of Ozone. Fourth, a discussion is presented that elucidates the utility of information concerning the ground state resonance structure of Mg water complexes with and without the presences of Ozone. This discussion also suggests procedures for the construction of permittivity functions that are in terms of reduced sets of phenomenological parameters. Finally, a conclusion is given summarizing the significance of modeling the dielectric response of molecular clusters relative to monitoring of water contamiants in practice.

Example of the Significance of Iron and Manganese Concentrations in Water and of Their Interaction with Ozone

New York City's water reservoirs, like all other cities upland water storage systems, have a continuous or occasional water quality problem when the two primary parameters of color colloids and turbidity inert particulates exceed the desirable limits. As these color colloidal particles are the result of decaying vegetation, the accompanying consequence is higher concentrations of both iron and manganese in the water, as both metals are present in the original vegetation and thereby in the color colloids resulting from the decay. Iron, of course, is present in much higher concentrations than manganese.

As the above mentioned water quality parameters are present in relatively low concentrations in typical upland water supply reservoirs, and as the size of all these particulates

are very small, the traditionally used water treatment of coagulation, flocculation, coarse dual media filtration would not only prove inefficient, but it would also require an addition of a disproportional amount of chemicals resulting in a large amount of a chemical sludge requiring disposal. Therefore, the diatomaceous earth filter media with their much smaller size of media particles and the resulting much smaller pore sizes, would be the most suitable filtering media for the treatment of these specific water pollutants requiring removal. Additionally, since the only chemical being added to the process is more diatomaceous earth, and as about 85 percent or more of the total DE material is being recovered and recycled in every run cycle, the resulting sludge is of a considerably lesser quantity and much more innocuous in its disposal.

The preozonation step added prior to the DE process has as its aim the oxidation of the soluble ionized ferric and manganic tiny particulates, therefore resulting in insoluble colloids of ferrous and manganous compounds. These can then be filtered out by the DE process much more efficiently, resulting in a desirable reduction of the iron and manganese concentrations, which are harmful to health, in addition to color and turbidity units reduction.

Therefore, as color levels in the water supply quality are closely correlated to both the turbidity and the iron and manganese concentrations, in modeling the preozonation, DE filtration process there seemed to be no statistical need to also include color as an additional modeling parameter. A multiparameter multiple regression analysis of the NYC pilot test data, which included color data as well, verified this assumption.

Calculation of Vibrational Spectra using DFT

As in previous studies [9,10,11] the formal mathematical structure underlying DFT calculations is included here for purposes of completeness. A brief description of this mathematical structure is as follows.

The DFT software GAUSSIAN09 (G09) can be used to compute an approximation of the IR absorption spectrum of a molecule or molecules [12]. This program calculates vibrational frequencies by determining second derivatives of the energy with respect to the Cartesian nuclear coordinates, and then transforming to mass-weighted coordinates at a stationary point of the geometry [13]. The IR absorption spectrum is obtained using density functional theory to compute the ground state electronic structure in the Born-Oppenheimer approximation using Kohn-Sham density functional theory [14-18]. GAUSSIAN uses specified orbital basis functions to describe the electronic wavefunctions and density. For a given set of nuclear positions, the calculation directly gives the electronic charge density of the molecule, the potential energy V, and the displacements in Cartesian coordinates of each atom. The procedure for vibrational analysis followed in GAUSSIAN is that described in [19]. Reference [20] presents a fairly detailed review of this procedure. A brief description of this procedure is as follows.

The procedure followed by GAUSSIAN is based on the fact the vibrational spectrum depends on the Hessian matrix $\mathbf{f}_{CART}$, which is constructed using the second partial derivatives of the potential energy V with respect to displacements of the atoms in Cartesian coordinates. Accordingly, the elements of the $3N$ x $3N$ matrix $\mathbf{f}_{CART}$ are given by

$$f_{CART ij} = \left(\frac{\partial^2 V}{\partial \xi_i \partial \xi_j} \right)_0 \qquad (1)$$

where $\{\xi_1, \xi_2, \xi_3, \xi_4, \xi_5, \xi_6, ..., \xi_{3N}\} = \{\Delta x_1, \Delta y_1, \Delta z_1, \Delta x_2, \Delta y_2, \Delta z_2, ..., \Delta z_N\}$, which are displacements in Cartesian coordinates, and N is the number of atoms. As discussed above, the zero subscript in Eq.(1) indicates that the derivatives are taken at the equilibrium positions of the atoms, and that the first derivatives are zero. Given the Hessian matrix defined by Eq.(1) the operations for calculation of the vibrational spectrum require that the Hessian matrix Eq.(1) be transformed to mass-weighted Cartesian coordinates according to the relation

$$ f_{\text{MWC}ij} = \frac{f_{\text{CART}ij}}{\sqrt{m_i m_j}} = \left(\frac{\partial^2 V}{\partial q_i \partial q_j} \right)_0 \tag{2} $$

where $\{q_1, q_2, q_3, q_4, q_5, q_6, ..., q_{3N}\} = \{\sqrt{m_1}\Delta x_1, \sqrt{m_1}\Delta y_1, \sqrt{m_1}\Delta z_1, \sqrt{m_2}\Delta x_2, \sqrt{m_2}\Delta y_2, \sqrt{m_2}\Delta z_2, ..., \sqrt{m_N}\Delta z_N\}$ are the mass-weighted Cartesian coordianates. GAUSSIAN computes the energy second derivatives Eq.(2), thus computing the forces for displacement perturbations of each atom along each Cartesian direction. The first derivatives of the dipole moment with respect to atomic positions $\partial \vec{\mu} / \partial \xi_i$ are also computed. Each vibrational eigenmode leads to one peak in the absorption spectrum, at a frequency equal to the mode's eigenfrequency ν_{n0}. The absorption intensity corresponding to a particular eigenmode n whose eigenfrequency is ν_{n0} is given by

$$ I_n = \frac{\pi}{3c} \left| \sum_{i=1}^{3N} \frac{\partial \vec{\mu}}{\partial \xi_i} l_{\text{CART}in} \right|^2, \tag{3} $$

where $\mathbf{l}_{\text{CART}}$ is the matrix whose elements are the displacements of the atoms in Cartesian coordinates. The matrix $\mathbf{l}_{\text{CART}}$ is determined by the following procedure. First,

$$ \mathbf{l}_{\text{CART}} = \mathbf{M} \mathbf{l}_{\text{MWC}} , \tag{4} $$

where $\mathbf{l}_{\text{MWC}}$ is the matrix whose elements are the displacements of the atoms in mass-weighted Cartesian coordinates and $\mathbf{M}$ is a diagonal matrix defined by the elements

$$ M_{ii} = \frac{1}{\sqrt{m_i}} . \tag{5} $$

Proceeding, $\mathbf{l}_{\text{MWC}}$ is the matrix needed to diagonalize $\mathbf{f}_{\text{MWC}}$ defined by Eq.(2) such that

$$ (\mathbf{l}_{\text{MWC}})^{\text{T}} \mathbf{f}_{\text{MWC}} (\mathbf{l}_{\text{MWC}}) = \Lambda , \tag{6} $$

where Λ is the diagonal matrix with eigenvalues λ_i. The procedure for diagonalizing Eq.(6) consists of the operations

$$ \mathbf{f}_{\text{INT}} = (\mathbf{D})^{\text{T}} \mathbf{f}_{\text{MWC}} (\mathbf{D}) \tag{7} $$

and

$$ (\mathbf{L})^{\text{T}} \mathbf{f}_{\text{MWC}} (\mathbf{L}) = \Lambda , \tag{8} $$

where $\mathbf{D}$ is a matrix transformation to coordinates where rotation and translation have been separated out and $\mathbf{L}$ is the transformation matrix composed of eigenvectors calculated according

to Eq.(8). The eigenfrequencies in units of (cm^{-1}) are calculated using the eigenvalues λ_n by the expression

$$\nu_{n0} = \frac{\sqrt{\lambda_n}}{2\pi c} \, ,$$ (9)

where c is the speed of light. The elements of $\mathbf{l}_{CART}$ are given by

$$l_{CARTki} = \sum_{j=1}^{3N} \frac{D_{kj} L_{ji}}{\sqrt{m_j}} \, ,$$ (10)

where $k, i = 1, \ldots, 3N,$ and the column vectors of these elements are the normal modes in Cartesian coordinates.

The intensity Eq.(3) must then be multiplied by the number density of molecules to give an absorption-line intensity in the non-interacting molecule approximation. It follows that the absorption spectrum calculated by GAUSSIAN is a sum of delta functions, whose line positions and coefficients correspond to the vibrational-transition frequencies and the absorption-line intensities, respectively. In principle, however, these spectral components must be broadened and shifted to account for anharmonic effects such as finite mode lifetimes and inter-mode couplings.

Physical Significance of Quantum Mechanical Transition State for Molecular Transformation

A molecule in 3-dimensions has a total of 3N-6 normal mode vibrations. The Schrodinger equation for the harmonic oscillations of these normal modes has known solutions. The quantum mechanical spectrum of each of these vibrations is given in the harmonic approximation by the energies $E_n = (n+1/2)h\nu$, where n is a quantum number, h is Planck's constant, and ν is a vibration frequency given by $\nu = \sqrt{(k/m)}$, where k is the spring constant of the normal vibration and m is the effective mass contributed by those atoms vibrating in the normal mode. A molecule in stable equilibrium is characterized by all positive normal mode frequencies ν. But the definitive mathematical characteristic of a transition state is that it has all positive frequencies but one, which is imaginary. That is to say, (k/m) is a negative number. The vibration corresponding to an imaginary frequency is one in which the atoms are breaking away from bonds characteristic of chemical reactants and are moving towards those bonds characteristic of chemical products. Chemical reactions break bonds in the reactants, rearrange them and form new bonds in the products. The transition state is a particular geometric arrangement of the atoms in a chemical system, at the maximal peak of the energy surface separating reactants from products. In the transition state every normal vibration distortion but one, occurs within a stable energy minimum. But the one normal mode distortion of imaginary frequency occurs at an unstable energy maximum sending reactants toward products. The height of energy peak, the activation energy E_a, associated with the occurrence of a transition state determines the minimal energy accumulated by reactants to surmount the barrier separating reactants from products. In the Arrhenius formulation, the rate constant for the reaction is given by $\Gamma = A\,e^{-Ea/RT}$, where A is a constant, R is the ideal gas constant, and T is the absolute temperature. The common

occurrence is that a particular transition state mechanism for chemical reaction is associated with one imaginary frequency, and therefore a single mechanism of reaction. Much less commonly, an energy surface of multiple channels of reaction mechanism may give rise to correspondingly multiple of imaginary frequencies. But in any event, the transition state contains the energetic and geometric information that defines the transformation inherent within chemical reactions.

Ground State Resonance Structure of Mg Water Complexes
And of Their Interaction with Ozone

In this section are presented the results of computational investigations using DFT concerning Mg water complexes and their interaction with Ozone. These results include the relaxed or equilibrium configurations of Mg water complexes, their interaction with Ozone, and ground-state oscillation frequencies and IR intensities for different geometries of the interacting systems associated with stable structures, which are calculated by DFT according to the frozen phonon approximation. For these calculations geometry optimization and vibrational analysis was effected using the DFT model B3LYP [22, 23] and basis function 6-31G(2d,2p) [24, 25]. According to the specification of this basis function, (d,p) designates polarization functions having 1 set of d functions for heavy atoms and 1 set of p functions for hydrogen atoms [26].

In general the geometry of any given Mg water complex interacting with Ozone will depend on the electronic configuration of the Ozone, as well as the orientation of Ozone relative to the Mg complex [27-36].

Shown in Table 1 are geometries and energies of Mg water complexes with Ozone, before and after geometry optimization, and without the presence of a water solvent background. In addition, indicated in Table 1 are the numbers of imaginary frequencies associated with the optimized geometries, as well as those molecular configurations for which convergence could not be achieved for geometry optimization. Referring to Table 1, it is to be noted that the labeling of molecular configurations with "1," e.g., Mg2-4H2O-2O3a1 in contrast to Mg2-4H2O-2O3a, indicates that the Ozones are next each other, in contrast to opposite to each other.

Shown in Figs. 1 through 8 are IR spectra calculated for the optimized geometries shown in Table 1. Again, it must be noted that we consider for potential correlation with experimentally measured spectra only calculated spectra associated with stable structures, i.e., structures for which there are no imaginary frequencies. The IR intensities shown in these figures are given in the form of continuous spectrum representations of the spectra. Comparison of these figures shows relative changes of intensities for individual resonances for the various Mg water complexes and their interaction with Ozone. The continuous spectra shown in Figs. 1 through 8 are constructed using a superposition of essentially Lorenzian functions of various heights and widths, which have been fit to the discrete spectra, and which have been calculated using DFT. The discrete spectra calculated by DFT used for construction of these continuous spectra are given in Tables 2 through 9. This construction is applied within the GAUSSIAN program [12].

Shown in Table 10 are energies, geometries and charges for $Mg^{++} \cdot n(H_2O) \cdot m(O_3)$, with and without a water solvent background, after geometry optimization. The results shown in this table are only for those molecules where stationary points were found, i.e., convergence could be achieved for geometry optimization. Shown in Fig. 9 are continuous spectra for those molecules indicated in Table 10 having stationary points for geometry optimization. The discrete spectra calculated by DFT used for construction of these continuous spectra are given in Tables 11

through 17. Again, this construction is applied within the GAUSSIAN program [12].

Shown in Table 18 are energies, geometries, charges and continuous spectra for $Mg^{++} \cdot n(H_2O)$ after geometry optimization. The discrete spectra calculated by DFT used for construction of these continuous spectra are given in Tables 19 through 21.

Discussion

The DFT calculated absorption spectra given in Tables 2 through 21 provide two types of information for general analysis of dielectric response. These are the denumeration of ground state resonance modes and estimates of molecular level dielectric response structure. The construction of permittivity functions using the DFT calculated absorption spectra follows the same procedure as that applied for the construction of permittivity functions using experimentally measured absorption spectra, but with the addition of certain constraint conditions. Accordingly, construction of permittivity functions using either DFT or experimentally measured absorption spectra requires parameterizations that are in terms of physically consistent analytic function representations such as the Drude-Lorentz model. Although the formal structure of permittivity functions constructed using DFT and experimental measurements are the same, their interpretation with respect to parameterization is different for each case. Better interpretation of dielectric response of molecules on a macroscale can be achieved through correlation of resonance structure, which is experimentally observed, with spectra calculated by DFT. In principle, correlation of resonance structure would include the quantitative analysis of changes in signature features associated with the transition of the system from that of a low-density system of uncoupled molecule to that of systems consisting of molecules coupled to their molecular environment. Among these types of systems are molecular clusters of explosive molecules or individual explosive molecules having intermolecular coupling with their ambient environment, consisting of either bulk systems or individual molecules, which would include water complexes.

One approach for the construction of permittivity functions using DFT calculations, discussed previously [10,11], is that of a direct problem approach where dielectric response is estimated within the bounds of relatively well-defined adjustable parameters. Following this approach, a permittivity function is constructed using the DFT calculated absorption spectra under the condition that the calculated resonance locations are fixed, while resonance widths and number densities are assumed adjustable. With respect to this approach, reference is made to Figs. 1 through 9, and inserts of Table 18, which show continuous spectra consisting of a superposition of essentially Lorenzian functions of various heights and widths, constructed using discrete spectra. Although the primarily purpose of this type of construction within GAUSSIAN is for the purpose of enhanced visualization of spectral features, it is significant to note that this operation represents, at some level, a zeroth-order estimation of the characteristic scaling and widths of resonances contributing the dielectric response, i.e., permittivity function. For qualitative comparison of spectral features this type of zeroth-order estimate should be sufficient. For the construction of permittivity functions to be used for quantitative simulations, it is more appropriate, however, to assume the characteristic scaling and widths of DFT calculated

8

resonances as adjustable parameters, i.e., parameters to be assigned values according to additional information.

Following an approach for construction of permittivity functions using DFT, which assumes the characteristic scaling and widths of resonances as adjustable parameters, inverse methods of analysis can be adopted. Accordingly, permittivity functions can be constructed using superpositions of Lorenzian functions that are in terms of reduced sets of phenomenological scaling and widths of resonances. This approach should consider, in principle, the sensitivity of reflectivity, as would be measured by a specific detection design (see reference [9]), with respect to variation in values of the associated phenomenological scaling and widths of resonances.

It must be emphasized again here, as in previous studies [10,11], that one purpose of DFT calculated spectra, related to practical application and extremely important for interpretation signature features and the design of detection or monitoring systems, is the quantitative analysis of the inherent limitation on levels of detection associated with various types of detection strategies. With respect to the purpose of examining inherent limitations on monitoring of water contaminants, the dominant features of response spectra that are calculated using DFT provide a foundation for establishing what level of detection is achievable in the absence of instrumental and environmental factors associated with detection. Accordingly, the approach presented here, for construction of permittivity functions, provides a specific application of DFT. For any given water contaminant, e.g., metal-water complex, and frequency range of the incident electromagnetic wave, DFT can calculate a set of response signatures that are each characterized by an excitation frequency, magnitude and width. These response signatures must then be adjusted parametrically to construct permittivity functions. Accordingly, parameter adjustment with respect to a given set of experimental measurements, which would entail parameter optimization and sensitivity analysis, will determine what types of signature structure are recoverable at the level of detection for a given detector design.

Finally, the DFT calculations presented here were performed using the DFT software GAUSSIAN. With respect to the approach presented here for construction of permittivity functions, these calculations represent results of numerical experiments with the "numerical apparatus" GAUSSIAN, which has associated with it specific discrete numerical representations and associated approximations. Again, an underlying factor supporting the construction of permittivity functions using DFT calculated spectra is that the associated software technology has evolved to a point of maturity where dielectric response to electromagnetic excitation can be determined quantitatively for large molecular systems.

Conclusion

The calculations of ground state resonance structure associated with Mg water complexes and their interaction with Ozone using DFT are meant to serve as reasonable estimates of molecular level response characteristics, providing interpretation of dielectric response features, for subsequent adjustment relative to experimental measurements and additional constraint based on molecular structure theory. With respect to spectroscopic methods for monitoring levels of water contamination, i.e., different types of detection strategies and their associated algorithms for post-processing of measurements, the calculated resonance spectra presented here serve the purpose of simulating detector designs for detection of water contaminants. That is to say, for detection of spatially distributed water complexes that correlate with different types of

contaminants, these spectra can be assumed as a reasonable estimate of dielectric response for purposes of the practical detection.

Acknowledgement

References
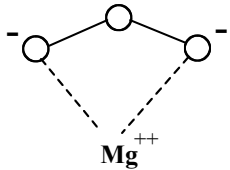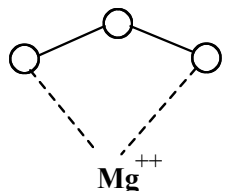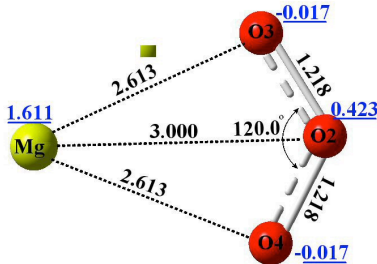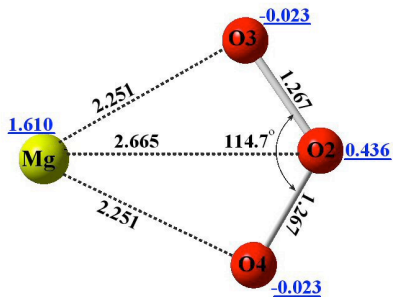
[1]   B. M. Rice and C. F. Chabalowski, "Ab Initio and Nonlocal Density Functional Study of 1,3,5-Trinitro-s-triazine (RDX) Conformers,``J. Phys. Chem., **101**, 8720 (1997).

[2]   Y. Chen, H. Liu, Y. Deng, D. Schauki, M. J. Fitch, R. Osiander, C. Dodson, J. B. Spicer, M. Shur, and X.-C. Zhang, "THz spectroscopic investigation of 2,4-dinitrotoluene," Chemical Physics Letters, **400**, 357-361 (2004).

[3]   D. G. Allis, D. A. Prokhorova, and T. M. Korter, "Solid-State Modeling of the Terahertz Spectrum of the High Explosive HMX," J. Phys. Chem. A., **110**, 1951-1959 (2006).

[4]   D.G. Allis and T. M. Korter, "Theoretical Analysis of the Terahertz Spectrum of the High Explosive PETN," Chem. Phys. Chem., **7**, 2398 (2006).

[5]   J. Chen, Y. Chen, H. Zhao, G. J. Bastiaans, and X.-C. Zhang, Opt. Exp., **15**, 11763 (2007).

[6]   M.R. Leahy-Hoppa, M.J. Fitch, X. Zheng, L.M. Hayden, and R. Osiander, "Wideband terahertz spectroscopy of explosives," Chemical Physics Letters **434**, 227-230 (2007).

[7]   J. Hooper, E. Mitchell, C. Konek, and J. Wilkinson, "Terahertz spectroscopy techniques for explosives detection," Chem. Phys. Lett., **467**, 309 (2009).

[8]   M.R. Leahy-Hoppa, M.J. Fitch, and R. Osiander,"Terahertz spectroscopy techniques for explosives detection," Anal. Bioanal. Chem., **395**, 247 (2009).

[9]   A. Shabaev, S. G. Lambrakos, N. Bernstein, V. L. Jacobs and D. Finkenstadt, "A General Framework for Numerical Simulation of Improvised Explosive Device (IED)-Detection Scenarios Using Density Functional Theory (DFT) and Terahertz (THz) Spectra," Appl. Spectroscopy, **65**, 409 (2011).

[10]   A. Shabaev, S.G., Lambrakos, N. Bernstein, V. Jacobs, D. Finkenstadt, "THz Dielectric Properties of High Explosives Calculated by Density Functional Theory for the Design Of Detectors," Journal of Materials Engineering and Performance, DOI: 10.1007/s11665 011-9857-8, 20 (9), 2011, p.1536.
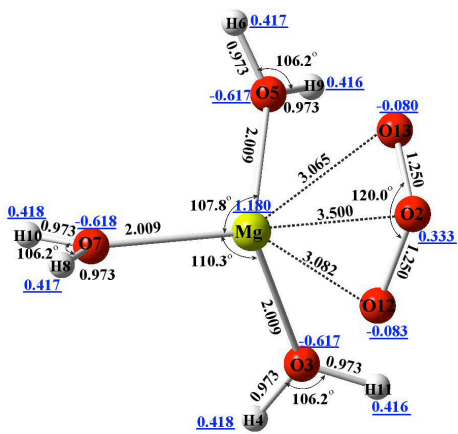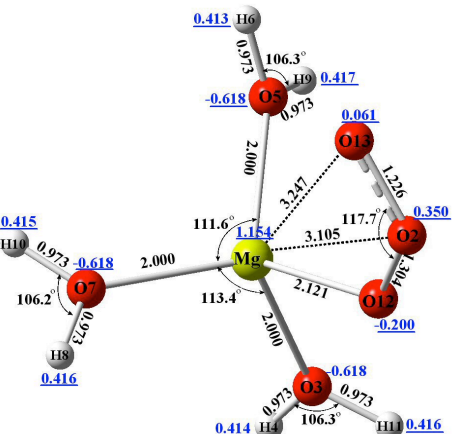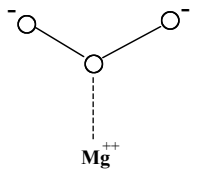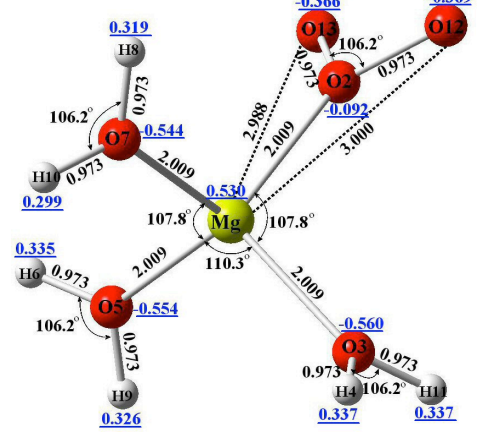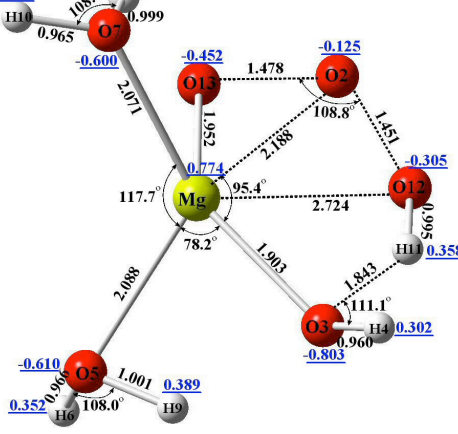
[11]   L. Huang, A. Shabaev, S.G. Lambrakos, N. Bernstein, V. Jacobs, D. Finkenstadt, L. Massa, "Dielectric Response of High Explosives at THz Frequencies Calculated Using Density Functional Theory," Journal of Materials Engineering and Performance, 2011, DOI: 10.1007/s11665-011-0020-3.

[12]   M. J. Frisch, G. W. Trucks, H. B. Schlegel, G. E. Scuseria, M. A. Robb, J. R. Cheeseman, G. Scalmani, V. Barone, B. Mennucci, G. A. Petersson, H. Nakatsuji, M. Caricato, X. Li, H. P. Hratchian, A. F. Izmaylov, J. Bloino, G. Zheng, J. L. Sonnenberg, M. Hada, M. Ehara, K. Toyota, R. Fukuda, J. Hasegawa, M. Ishida, T. Nakajima, Y. Honda, O. Kitao, H. Nakai, T. Vreven, J. A. Montgomery, Jr., J. E. Peralta, F. Ogliaro, M. Bearpark, J. J. Heyd, E. Brothers, K. N. Kudin, V. N. Staroverov, R. Kobayashi, J. Normand, K. Raghavachari, A. Rendell, J. C. Burant, S. S. Iyengar, J. Tomasi, M. Cossi, N. Rega, J. M. Millam, M. Klene, J. E. Knox, J. B. Cross, V. Bakken, C. Adamo, J. Jaramillo, R. Gomperts, R. E. Stratmann, O. Yazyev, A. J. Austin, R. Cammi, C. Pomelli, J. W. Ochterski, R. L. Martin, K. Morokuma, V. G. Zakrzewski, G. A. Voth, P. Salvador, J. J. Dannenberg, S. Dapprich, A. D. Daniels, Ö. Farkas, J. B. Foresman, J. V. Ortiz, J. Cioslowski, and D. J. Fox, Gaussian 09, Revision A.1, Gaussian, Inc., Wallingford CT, 2009.

[13]   A. Frisch, M. J. Frisch, F. R. Clemente and G. W. Trucks, *Gaussian 09 User's Reference,* Gaussian Inc., 2009, p, 105-106, online: www.gaussian.com/g_tech/g_ur/g09help.htm

[14]   P. Hohenberg and W. Kohn, "Inhomogeneous Electron Gas" Phys. Rev. **136**, B864, (1964).

[15]   W. Kohn and L. J. Sham, "Self-Consistent Equations Including Exchange and Correlation Effects" Phys. Rev. **140**, A1133 (1965).

[16]   R.O. Jones and O. Gunnarson, "The density functional formalism, its applications and prospects" Rev. Mod. Phys. **61**, 689 (1989).

[17]   W.W. Hager and H. Zhang, "A survey of nonlinear conjugate gradient methods," Pacific J. Optim., 2, p. 35-58 (2006).

[18]   R. M. Martin, *Electronic Structures Basic Theory and Practical Methods*, Cambridge University Press, Cambridge 2004, p. 25.

[19]   E. B. Wilson, J. C. Decius and P. C. Cross, *Molecular Vibrations* (McGraw-Hill, New York, 1955).

[20]   J.W. Ochterski, "Vibrational Analysis in Gaussian," help@gaussian.com, 1999.

[21]   C. A. D. Roeser and E. Mazur, "Light-Matter Interactions on Femtosecond Time Scale" in *Frontiers of Optical Spectroscopy*, eds. B. Di Bartolo and O. Forte, NATO Science Series v. 168 p. 29, Kluwer Academic Publishers, Dordrecht − Norwell, 2005; C. F.
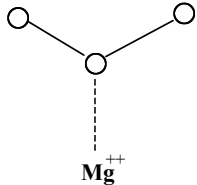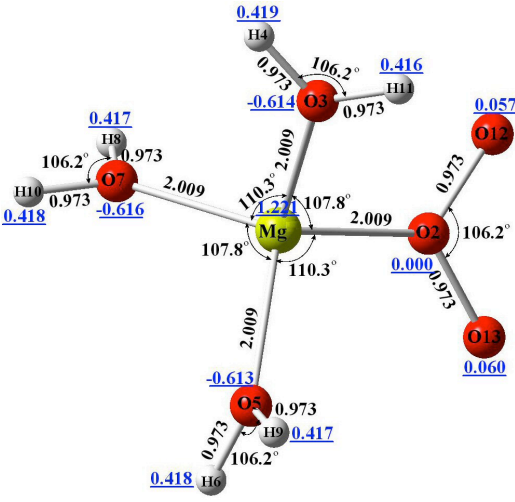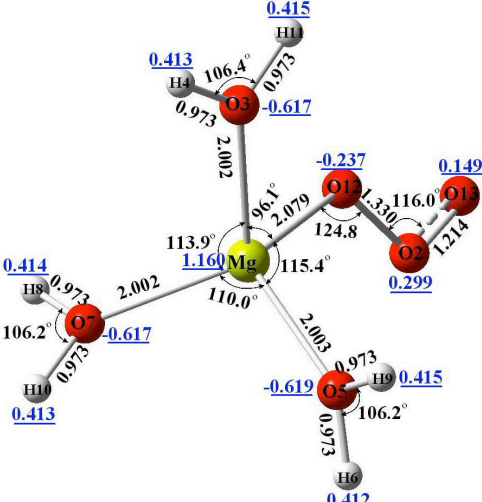
Bohren and D. R. Huffman, *Absorption and Scattering of Light by Small Particles* (Wiley-VCH Verlag, Weinheim, 2004).

[22] A. D. Becke, "Density-functional Thermochemistry. III. The Role of Exact Exchange", *J. Chem. Phys.* **98**, 5648-5652 (1993).

[23] B. Miehlich, A. Savin, H. Stoll and H. Preuss, "Results Obtained with the Correlation Energy Density Functionals of Becke and Lee, Yang and Parr", Chem. *Phys. Lett.* **157**, 200-206 (1989).

[24] A. D. McLean and G. S. Chandler, "Contracted Gaussian-basis sets for molecular calculations. 1. 2nd row atoms, Z=11-18," *J. Chem. Phys.*, **72** 5639-48 (1980).

[25] T. Clark, J. Chandrasekhar, G. W. Spitznagel and P. V. R. Schleyer, "Efficient diffuse function-augmented basis-sets for anion calculations. 3. The 3-21+G basis set for 1st-row elements, Li-F," *J. Comp. Chem.*, **4** 294-301, (1983).

[26] M. J. Frisch, J. A. Pople and J. S. Binkley, "Self-Consistent Molecular Orbital Methods. 25. Supplementary Functions for Gaussian Basis Sets," *J. Chem. Phys.*, **80** (1984) 3265-69.

[27] M. Adrian-Scotto, D. Vasileva, G. Mallet, D. Vasilescu, " About the Hydration of Mg^{++}: A Quantum DFT Study," Internet Electron. J. Mol. Des., 3, 400-411 (2004).

[28] M. anekata, F. Misaizu, K. Fuke, S. Iwata, K. Hashimoto, "Reactions of Singly Charged Alkaline-Earth Metal Ions with Water Clusters: Characteristic Size Distribution of Product Ions," J. Am. Chem. Soc., 117, 747-754 (1995).

[29] T.Dudev, J. A. Cowan, C. Lim, " Cometitive Binding in Magnesium Coodination Chemistry: Water versus Ligands of Biological Interest," J. Am. Chem. Soc., 121, 7665-7673 (1999).

[30] K. Fuke, F. Misaizu, M. Sanekata, K. Tsukamoto, S. Iwata, " Electronic structure and reactivity of $Mg^+(H_2O)_n$ cluster ions," Supplement to Z. Phys. D 26, S 180-182 (1993).

[31] M. Pavlov, P. E. M. Siegbahn, M. Sandström, "Hydration of Beryllium, Magnesium, Calcium, and Zinc Ions Using Density Functional Theory," J. Phys. Chem. A, 102, 219-228 (1998).

[32] M. Adrian-Scotto, G. Mallet, D. Vasilescu, " Hydration of Mg^{++}: a quantum DFT and ab initio HF study," J. Mol. Str.: THEOCHEM, 728, 231-242 (2005).

[33] B. M. Reinhard, G. Niedner-Schatteburg, " ab initio treatment of magnesium water cluster anions $[Mg,nH_2O]^-$, n≤ 11," Phys. Chem. Chem. Phys., 5, 1970-1980 (2003).

[34] B. M. Reinhard, A. Lagutschenkov, G. Niedner-Schatteburg, "Ab initio study of
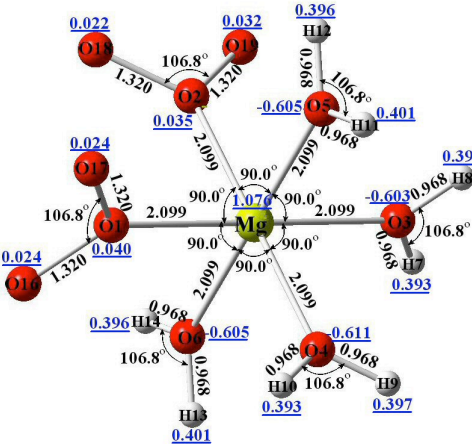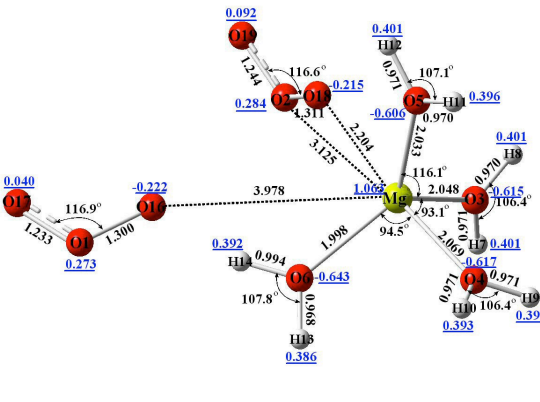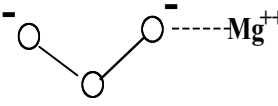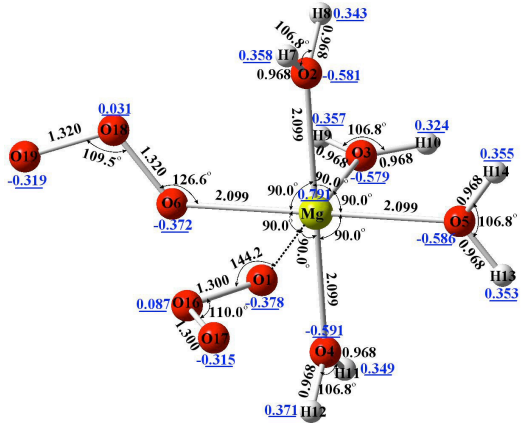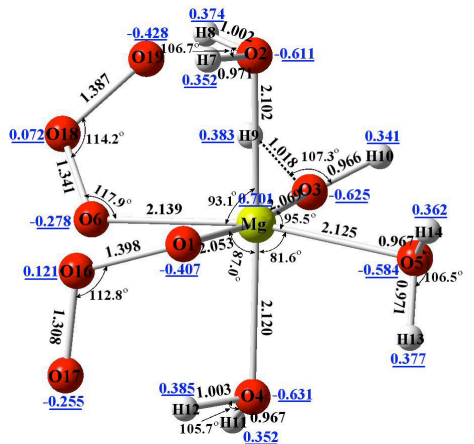
[Mg,nH$_2$O]$^-$ reactive decay products: structure and stability of magnesium oxide and magnesium hydroxide water cluster anions [MgO,(n-1)H$_2$O]$^-$, [HMgOH,(n-1)H$_2$O]$^-$ and [Mg(OH)$_2$,(n-2)H2O]$^-$," Phys. Chem. Chem. Phys., 6, 4268-4275 (2004).

[35]　　H. Watanabe, S. Iwata, K. Hashimoto, F. Misaizu, K. Fuke, "Molecular Orbital Studies of the Structures and Reactions of Singly Charged Magnesium Ion with Water Clusters, Mg$^+$(H$_2$O)n," J. Am. Chem. Soc., 117, 755-763 (1995).

[36]　　H. Watanabe, S. Iwata, "Theoretical assignments of the photo-dissociation excitation spectra of Mg$^+$ ion complexes with water clusters: Multi-reference CI studies," J. Chem. Phys., 108, 10078-10083 (1998).
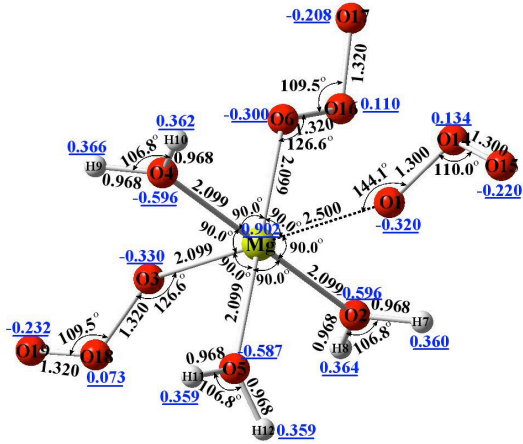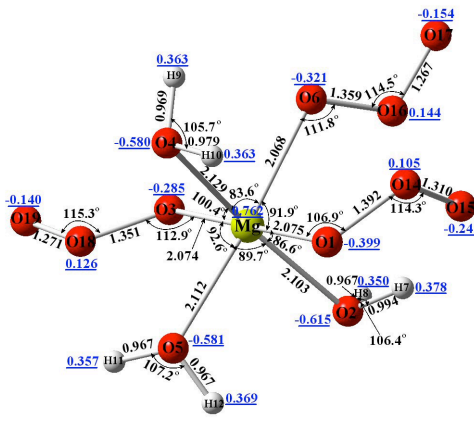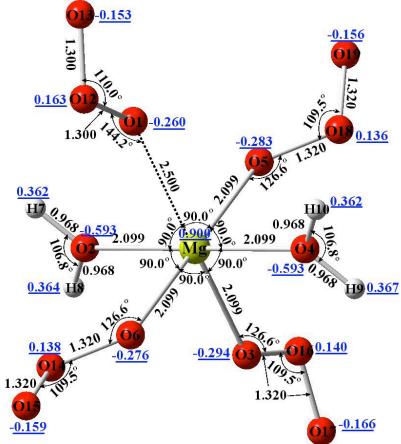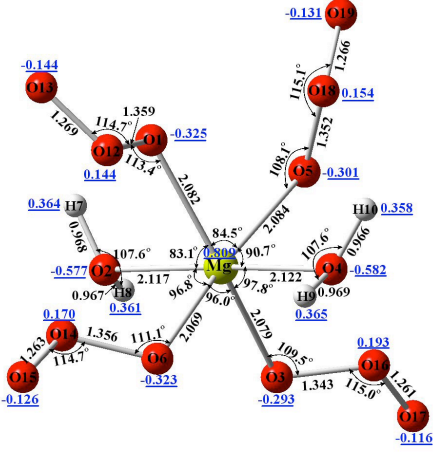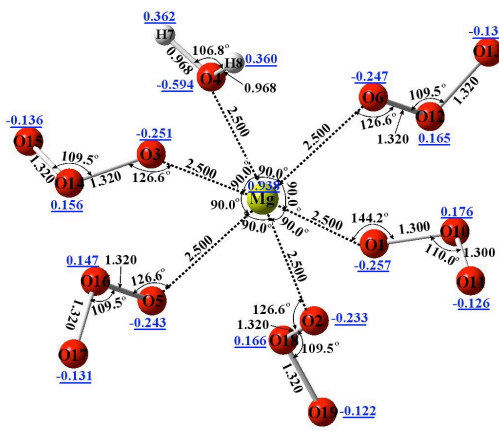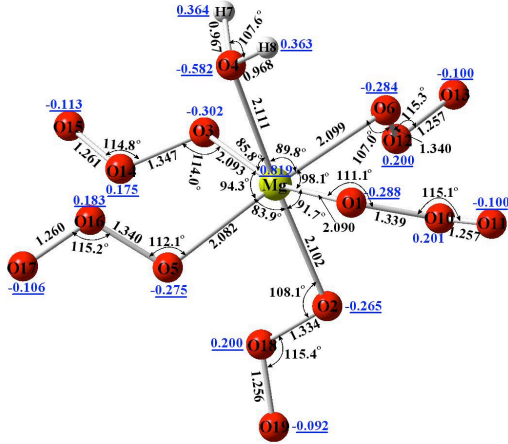
Table 1. Energies and charges for $Mg^{++} \cdot n(H_2O) \cdot m(O_3)$ before and after geometry optimization.
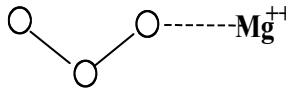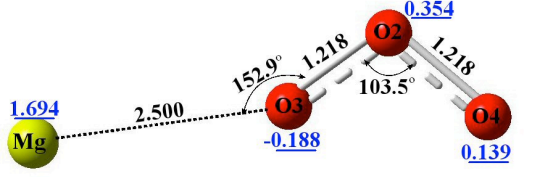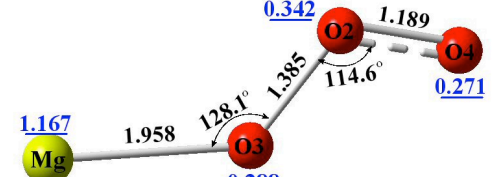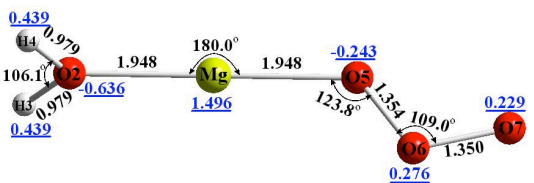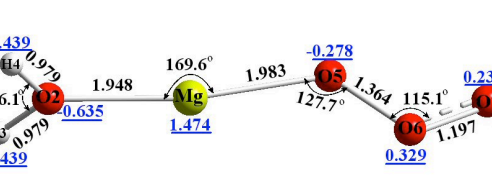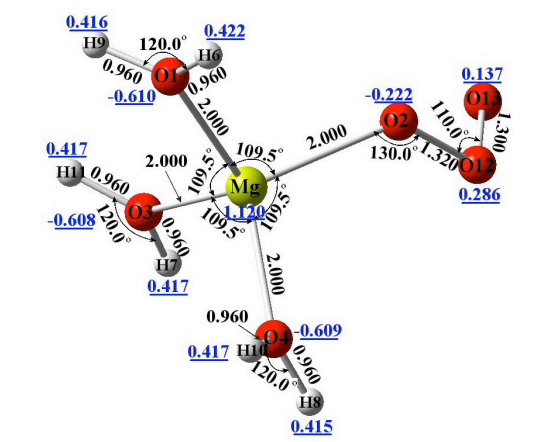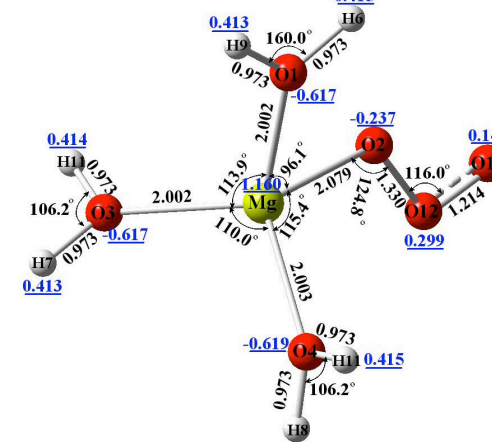
A	Start Geometry	Opt Geometry
	No charges in complex	
Mg2-1O3a	Convergence failure	
Mg2-1H2O-1O3a	Convergence failure	
Mg2-2H2O-1O3a	Stationary point found with 4 imaginary frequencies	
Mg2-3H2O-1O3a	Convergence failure	
Mg2-4H2O-1O3a	Stationary point found with 6 imaginary frequencies	
Mg2-5H2O-1O3a	Convergence failure	
Mg2-4H2O-2O3a	Convergence failure	
Mg2-4H2O-2O3a1	Convergence failure	
Mg2-3H2O-3O3a	Convergence failure	
Mg2-2H2O-4O3a	Convergence failure	
Mg2-1H2O-5O3a	Convergence failure	
Mg2-6O3a	Convergence failure	
	2 positive charges in complex	
Mg-1O3a	 E= -424.7175 a.u.	 E= -424.7322 a.u.
Mg-1H2O-1O3a	Stationary point found with 1 imaginary frequencies	
Mg-2H2O-1O3a	Stationary point found with 2 imaginary frequencies	
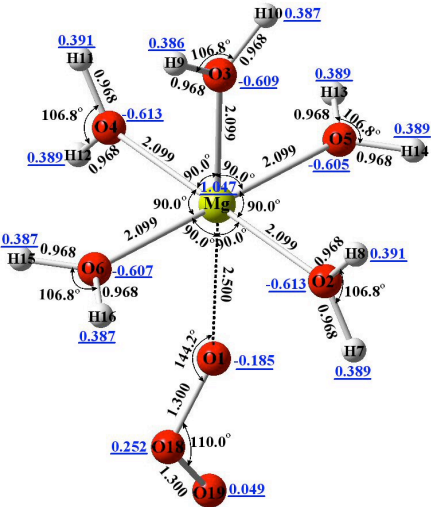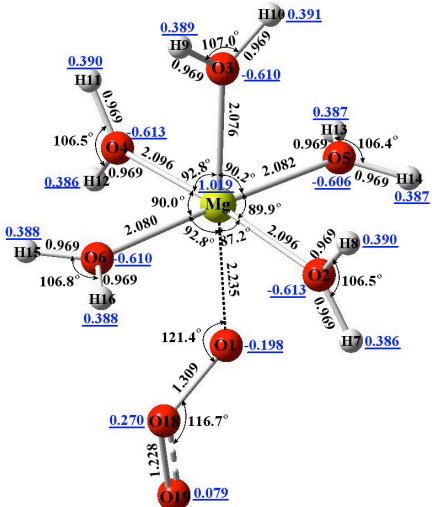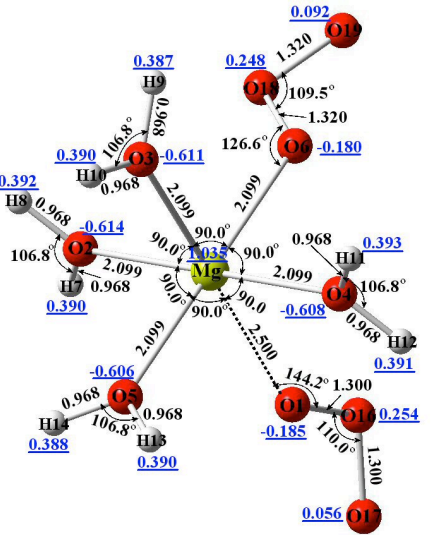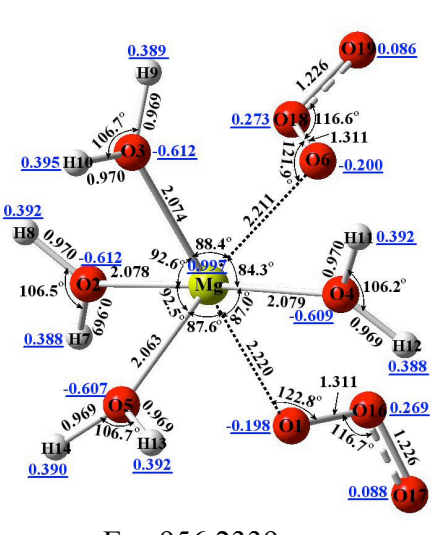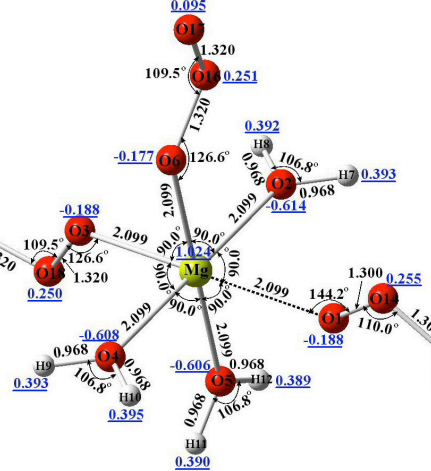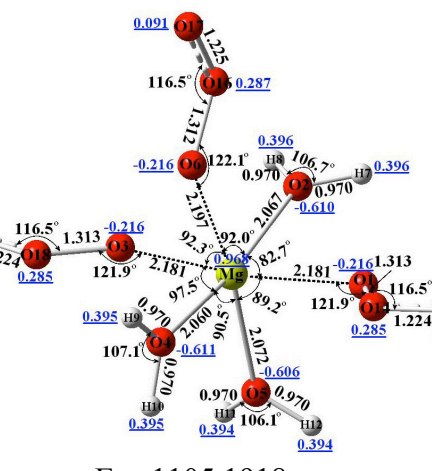
Mg-3H2O-1O3a	 E= -654.3002 a.u.	 E= -654.3201 a.u.
Mg-4H2O-1O3a	Stationary point found with 3 imaginary frequencies	
Mg-5H2O-1O3a	Stationary point found with 2 imaginary frequencies	
Mg-4H2O-2O3a	Stationary point found with 6 imaginary frequencies	
Mg-4H2O-2O3a1	Convergence failure	
Mg-3H2O-3O3a	Stationary point found with 8 imaginary frequencies	
Mg-2H2O-4O3a	Stationary point found with 8 imaginary frequencies	
Mg-1H2O-5O3a	Stationary point found with 6 imaginary frequencies	
Mg-6O3a	Stationary point found with 6 imaginary frequencies	

B	**Start Geometry**	**Opt Geometry**
	No charges in complex	
Mg2-1O3b	Convergence failure	
Mg2-1H2O-1O3b	Convergence failure	
Mg2-2H2O-1O3b	Stationary point found with 3 imaginary frequencies	
Mg2-3H2O-1O3b	 E= -654.8059 a.u.	 E= -655.0092 a.u.
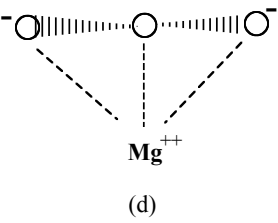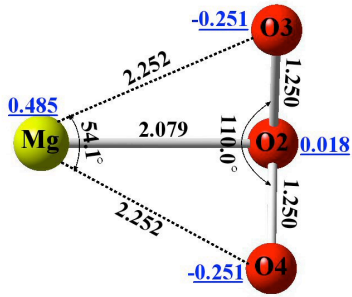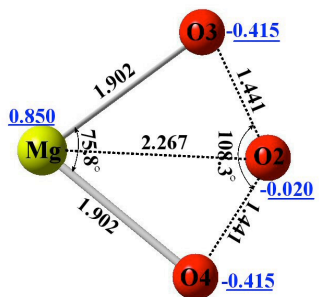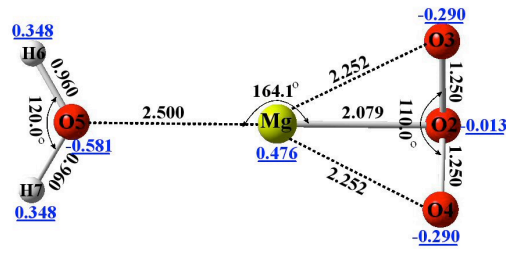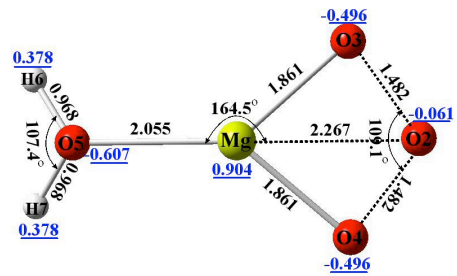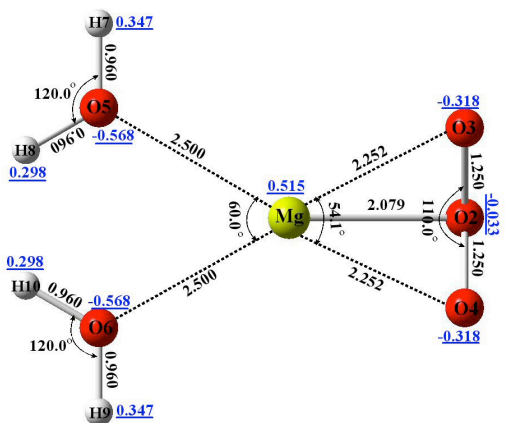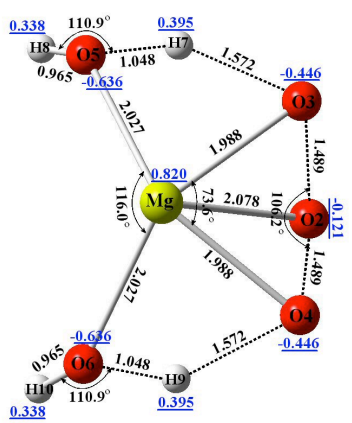
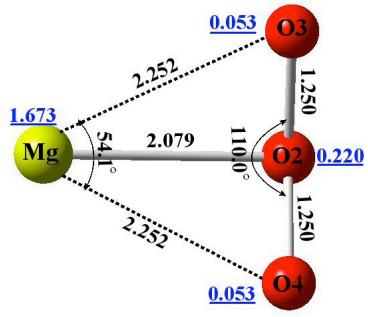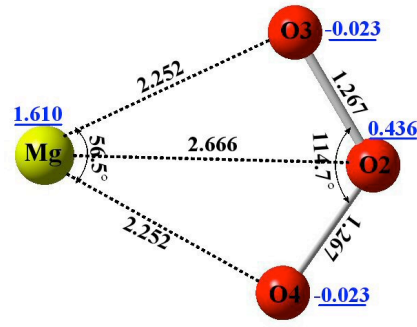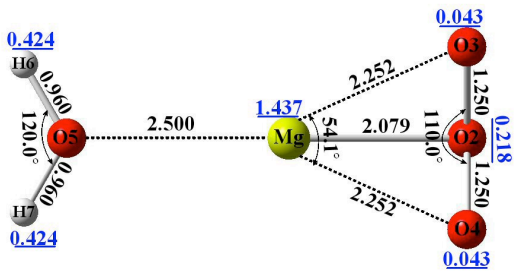|	
Mg2-4H2O-1O3b	Convergence failure
Mg2-5H2O-1O3b	Convergence failure
Mg2-4H2O-2O3b	Stationary point found with 11 imaginary frequencies
Mg2-4H2O-2O3b1	Convergence failure
Mg2-3H2O-3O3b	Convergence failure
Mg2-2H2O-4O3b	Convergence failure
Mg2-1H2O-5O3b	Convergence failure
Mg2-6O3b	Convergence failure
	2 positive charges in complex
Mg-1O3b	Stationary point found with 1 imaginary frequencies
Mg-1H2O-1O3b	Stationary point found with 2 imaginary frequencies
Mg-2H2O-1O3b	Stationary point found with 4 imaginary frequencies
Mg-3H2O-1O3b	 E= -654.2543 a.u. E= -654.3221 a.u.
Mg-4H2O-1O3b	Stationary point found with 8 imaginary frequencies
Mg-5H2O-1O3b	Stationary point found with 3 imaginary frequencies
Mg-4H2O-2O3b	Stationary point found with 4 imaginary frequencies
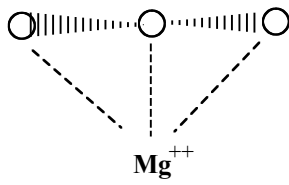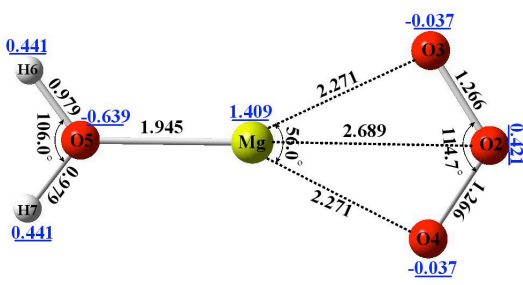
Mg-4H2O-2O3b1	E= -956.1261 a.u.	E= -956.2325 a.u
Mg-3H2O-3O3b	Stationary point found with 6 imaginary frequencies	
Mg-2H2O-4O3b	Stationary point found with 7 imaginary frequencies	
Mg-1H2O-5O3b	Stationary point found with 4 imaginary frequencies	
Mg-6O3b	Stationary point found with 6 imaginary frequencies	

C	**Start Geometry**	**Opt Geometry**
	No charges in complex	
Mg2-1O3c	Convergence failure	
Mg2-1H2O-1O3c	Convergence failure	
Mg2-2H2O-1O3c	Convergence failure	
Mg2-3H2O-1O3c	Convergence failure	
Mg2-4H2O-1O3c	Convergence failure	
Mg2-5H2O-1O3c	Convergence failure	
Mg2-4H2O-2O3c	Convergence failure	
Mg2-4H2O-2O3c1		

	E= -956.7663 a.u.	E= -956.9107 a.u.
Mg2-3H2O-3O3c	E= -1105.8013 a.u.	E= -1105.8748 a.u.
Mg2-2H2O-4O3c	E= -1254.7905 a.u.	E=-1254.8412 a.u.
Mg2-1H2O-5O3c	E= -1403.6935 a.u.	E= -1403.8146 a.u.
Mg2-6O3c	Convergence failure	

	2 positive charges in complex	
Mg-1O3c	E= -424.6833 a.u.	E= -424.7415 a.u.
Mg-1H2O-1O3c	E= -501.2678 a.u.	E= -501.2889 a.u.
Mg-2H2O-1O3c	Stationary point found with 1 imaginary frequencies	
Mg-3H2O-1O3c	E= -65.2861 a.u.	E= -654.3221 a.u.
Mg-4H2O-1O3c	Stationary point found with 1 imaginary frequencies	

Mg-5H2O-1O3c	E= -807.2645 a.u.	E= -807.2784 a.u.
Mg-4H2O-2O3c	Stationary point found with 1 imaginary frequencies	
Mg-4H2O-2O3c1	E= -956.2074 a.u.	E= -956.2339 a.u.
Mg-3H2O-3O3c	E= -1105.1498 a.u.	E= -1105.1918 a.u.

Mg-2H2O-4O3c	Convergence failure
Mg-1H2O-5O3c	Convergence failure
Mg-6O3c	Convergence failure

D	Start Geometry	Opt Geometry
(d)	**No charges in complex**	
Mg2-1O3d	E= -425.5056 a.u.	E= -425.5847 a.u.
Mg2-1H2O-1O3d	E= -501.421 a.u.	E= -502.05487 a.u.
Mg2-2H2O-1O3d	E= -578.3627 a.u.	E= -578.5279 a.u.

21

Mg2-3H2O-1O3d	Convergence failure
Mg2-4H2O-1O3d	Convergence failure
Mg2-5H2O-1O3d	Convergence failure
Mg2-4H2O-2O3d	Convergence failure
Mg2-4H2O-2O3d1	Convergence failure
Mg2-3H2O-3O3d	Convergence failure
Mg2-2H2O-4O3d	Convergence failure
Mg2-1H2O-5O3d	Convergence failure
Mg2-6O3d	Convergence failure
  Mg^{++}	**2 positive charges in complex**
Mg-1O3d	 E= -424.6468 a.u.	 E= -424.7322 a.u.
Mg-1H2O-1O3d	 E= -501.1693 a.u.	 E= -501.2821 a.u.

Mg-2H2O-1O3d	 E= -577.6438 a.u.	 E= -577.8103 a.u.
Mg-3H2O-1O3d	 E= -654.1885 a.u.	 E= -655.0092 a.u.
Mg-4H2O-1O3d	Convergence failure	
Mg-5H2O-1O3d	Convergence failure	
Mg-4H2O-2O3d	Convergence failure	
Mg-4H2O-2O3d1	Convergence failure	
Mg-3H2O-3O3d	Convergence failure	
Mg-2H2O-4O3d	Convergence failure	
Mg-1H2O-5O3d	Convergence failure	
Mg-6O3d	Convergence failure	
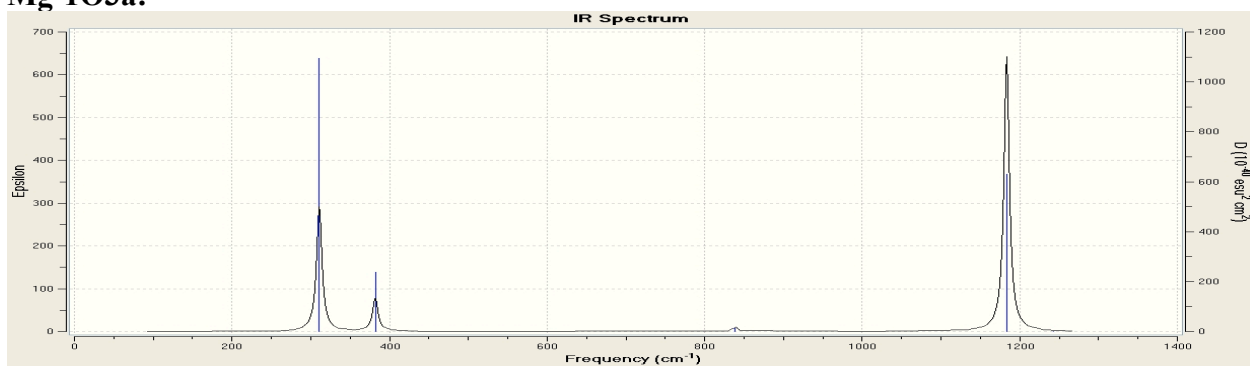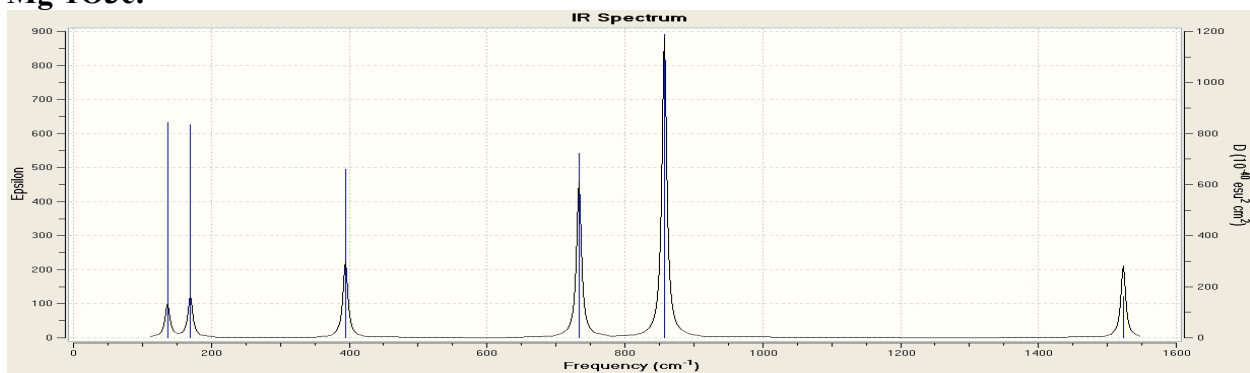
Mg-1O3a:
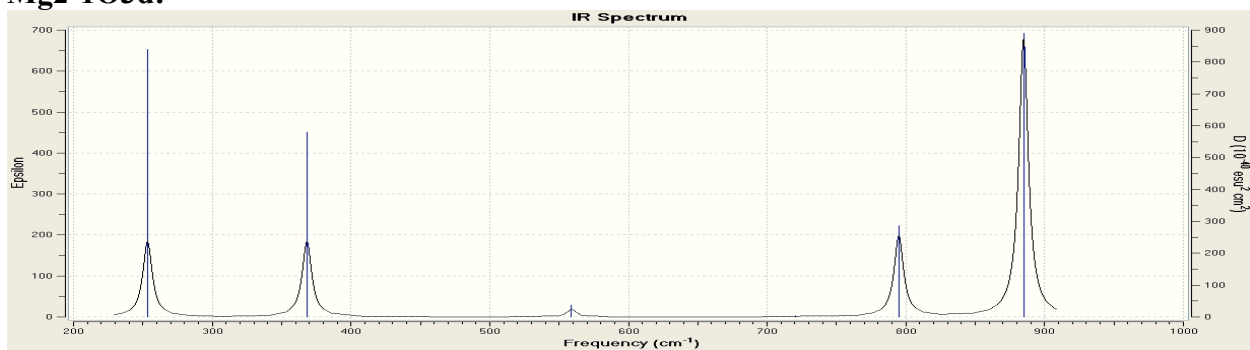
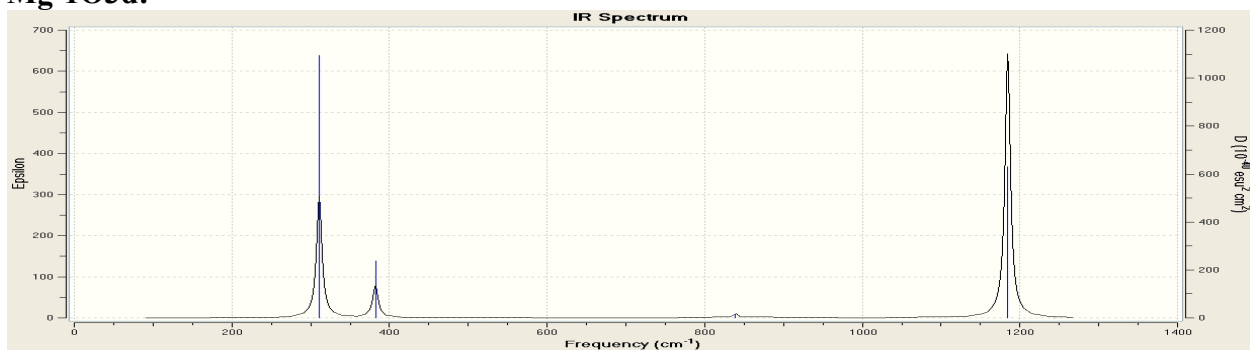

Mg-1O3c:

Mg2-1O3d:

Mg-1O3d:

Figure 1. IR intensity as a function of frequency calculated using DFT for Mg-1O3a, Mg-1O3c, Mg2-1O3d and Mg-1O3d according to frozen phonon approximation.

Table 2. Oscillation frequencies and IR intensities for Mg-1O3a, Mg-1O3c, Mg2-1O3d and Mg-1O3d (see Figure 1).

| Mg-1O3a:		Mg-1O3c:		Mg2-1O3d:		Mg-1O3d:	
Freq(1/cm)	Inten(KM/Mol)	Freq(1/cm)	Inten(KM/Mol)	Freq(1/cm)	Inten(KM/Mol)	Freq(1/cm)	Inten(KM/Mol)
116.205	0.0001	136.45	28.9002	253.3775	53.2699	115.6423	0.0001
310.7802	85.3035	169.5235	35.4807	368.2854	53.5242	310.8413	85.3145
381.886	22.8182	394.5152	65.2601	558.8165	5.3027	382.1582	22.8082
838.8505	2.9865	733.4482	132.7704	720.424	0.4702	839.2355	3.0036
1183.368	186.7998	857.2642	255.3212	794.8879	57.1939	1184.495	186.8046
1242.6531	0.0463	1523.0702	61.6723	884.8019	197.3157	1242.865	0.0441

Table 3. Oscillation frequencies and IR intensities for Mg-1H2O-1O3c, Mg2-1H2O-1O3d and Mg-1H2O-1O3d (see Figure 2).

Mg-1H2O-1O3c:		Mg2-1H2O-1O3d:		Mg-1H2O-1O3d:	
Freq(1/cm)	Inten(KM/Mol)	Freq(1/cm)	Inten(KM/Mol)	Freq(1/cm)	Inten(KM/Mol)
35.2435	3.548	36.1449	24.3721	45.8837	16.1652
40.3826	9.3614	46.2365	0.3992	46.9206	0
42.3326	6.6354	92.1743	21.6302	47.9865	8.7793
134.6235	18.1414	97.985	11.8493	109.0062	0.6869
163.9555	20.5552	299.5928	34.4886	241.4501	28.6075
305.3984	21.2473	318.8459	236.8339	367.434	12.8139
511.0872	385.7808	477.4425	23.6419	519.9559	389.4466
578.2117	69.1697	530.0858	31.2817	569.6581	78.1395
677.9882	123.7856	634.3446	2.5162	679.3558	98.5508
752.8746	118.5243	749.7093	99.7952	833.5256	5.9611
909.8004	265.9528	764.9348	36.3236	1194.7815	182.8975
1493.2677	58.4226	874.3908	16.3809	1250.973	0.5507
1682.9148	136.3366	1646.6492	113.2794	1683.0918	136.8131
3667.8477	297.6331	3783.145	61.1318	3661.135	288.7889
3722.3076	385.2499	3881.4927	167.7647	3714.2192	378.7432

Mg-1H2O-1O3c:
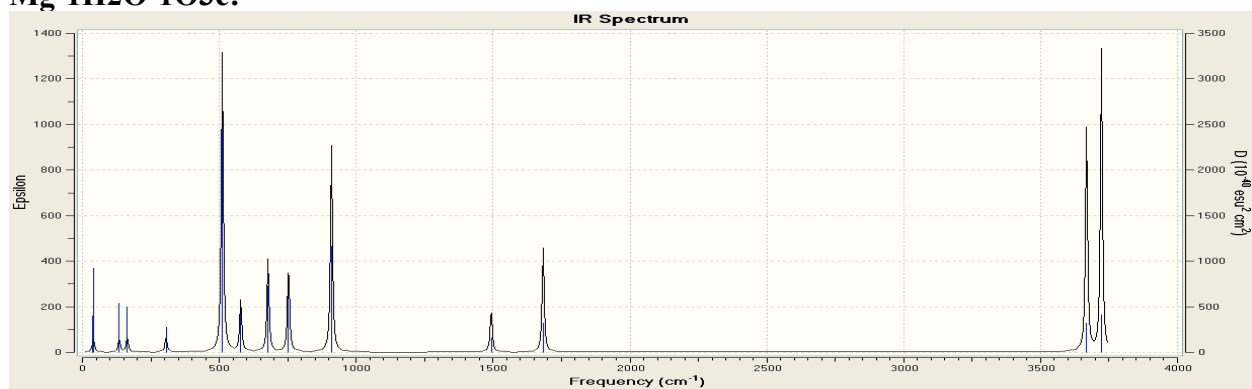
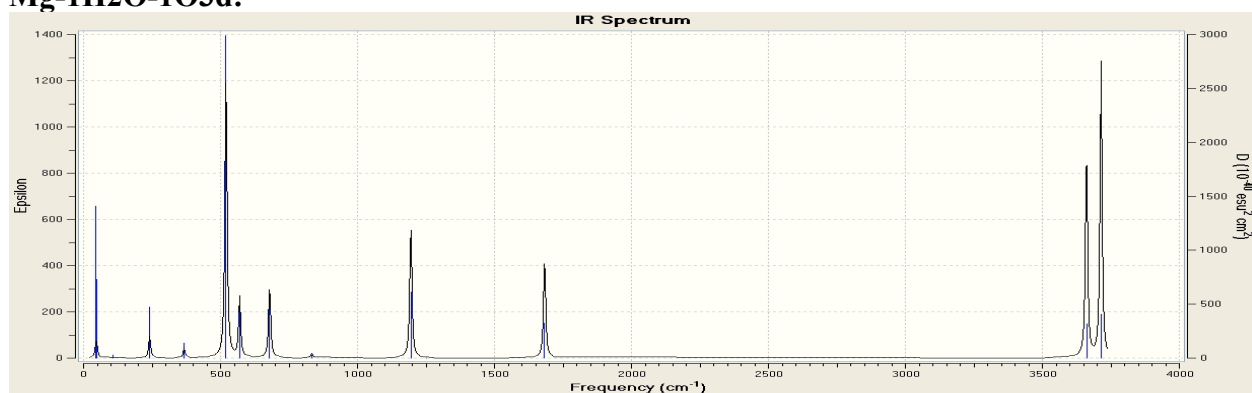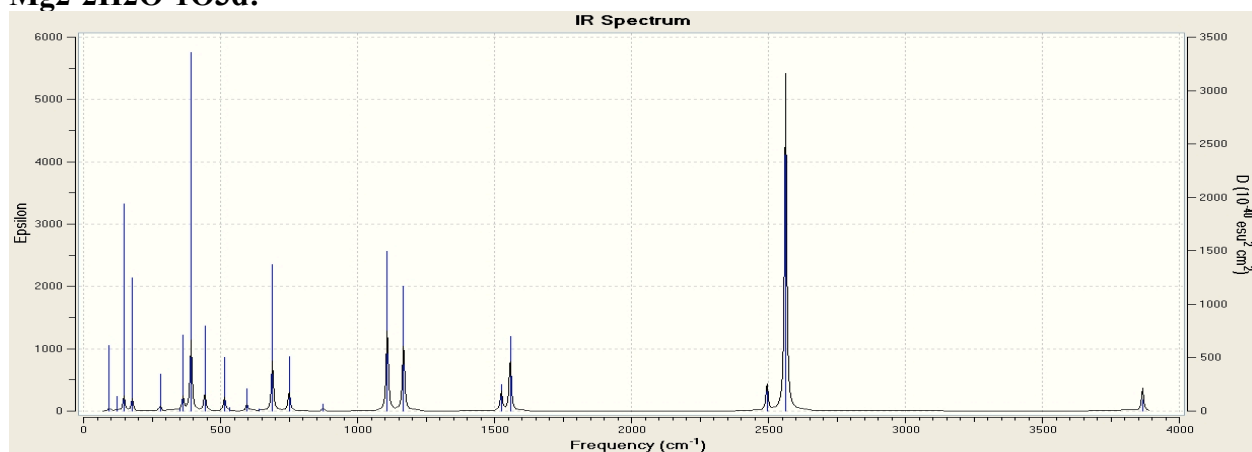**Mg2-1H2O-1O3d:**
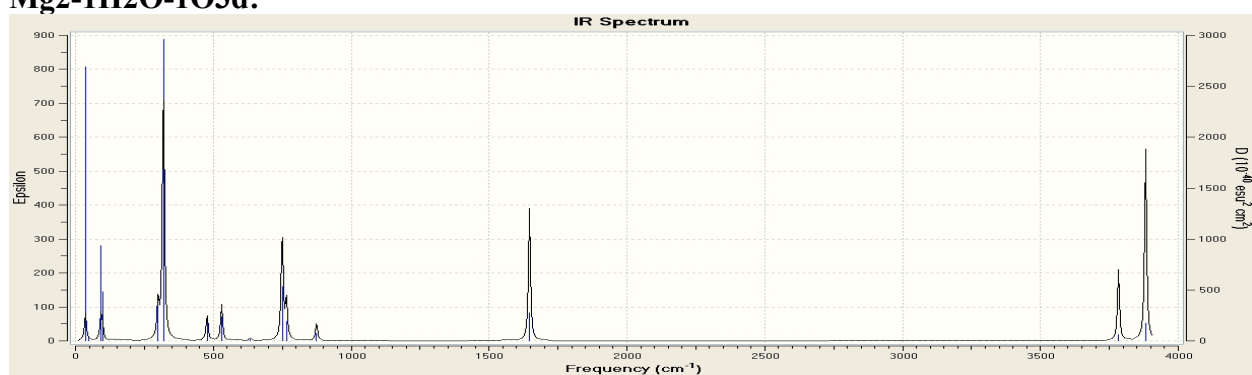
Mg-1H2O-1O3d:

Figure 2. IR intensity as a function of frequency calculated using DFT for Mg-1H2O-1O3c, Mg2-1H2O-1O3d and Mg-1H2O-1O3d according to frozen phonon approximation.

Mg2-2H2O-1O3d:
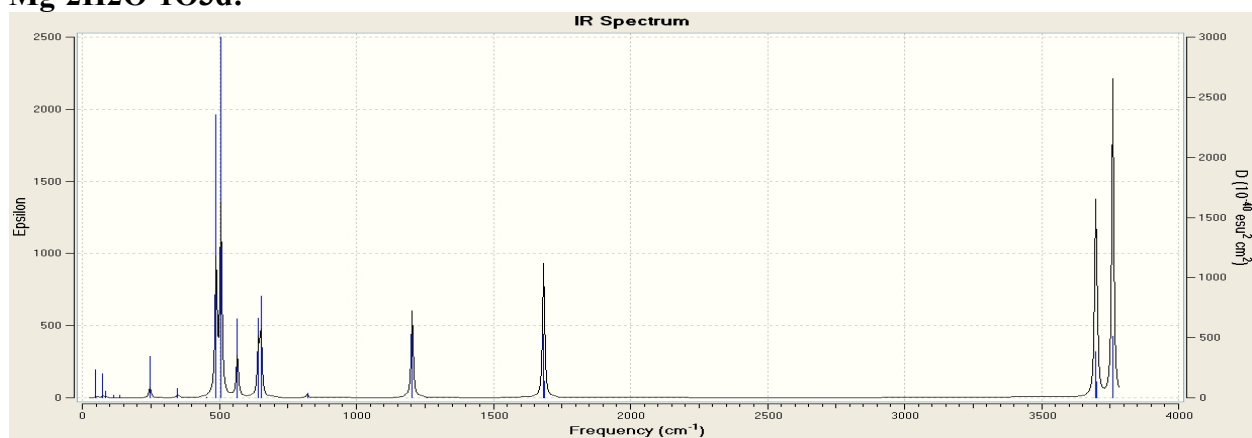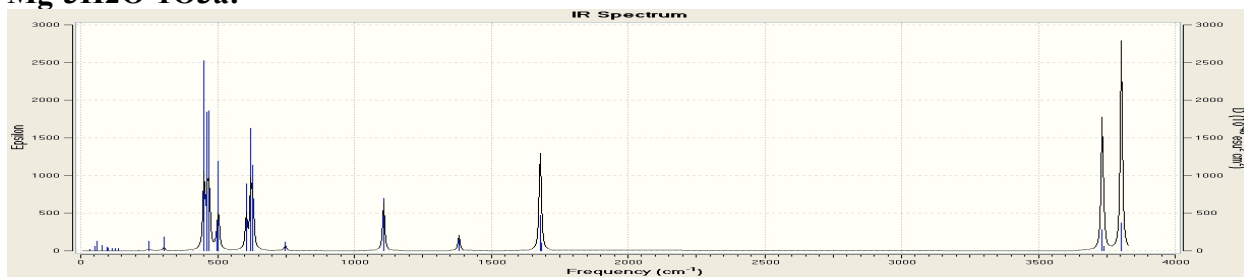

Mg-2H2O-1O3d:

Figure 3. IR intensity as a function of frequency calculated using DFT for Mg2-2H2O-1O3d and Mg-2H2O-1O3d according to frozen phonon approximation.
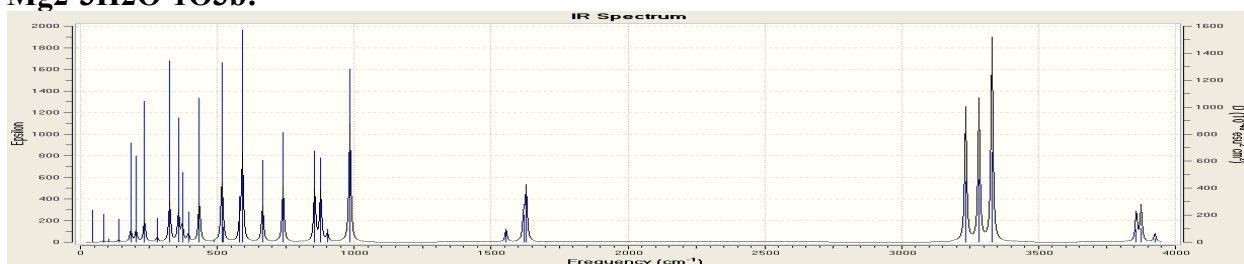
Table 4. Oscillation frequencies and IR intensities for Mg2-2H2O-1O3d and Mg-2H2O-1O3d (see Figure 3).

Mg2-2H2O-1O3d: **Mg-2H2O-1O3d:**

Freq(1/cm)	Inten(KM/Mol)	Freq(1/cm)	Inten(KM/Mol)
93.9378	14.4149	49.445	2.9078
124.0353	4.1803	51.7562	0.0018
147.4935	71.5839	73.8167	0.1948
177.8758	55.5878	74.9963	3.8061
279.7559	24.2964	84.0022	1.1702
353.2788	3.0285	112.943	0.5699
363.1929	64.9117	136.0564	0.7607
392.5141	330.0376	247.265	21.3213
442.64	88.3795	348.4936	6.7855
514.6127	64.5447	454.6057	0.5989
532.804	4.1138	488.1969	288.2866
596.9698	31.7084	505.8858	380.1182
639.3071	2.9389	565.9757	93.202
689.4696	236.901	642.6899	106.6827
750.4567	96.1587	651.8509	138.0039
874.7008	14.2223	821.0946	7.7609
1108.7642	415.2317	1203.7217	180.2606
1168.1742	342.3752	1257.4008	0.859
1524.9457	94.874	1682.8835	223.064
1557.5304	271.8739	1684.7209	59.6506
2494.8286	135.3197	3696.8979	355.2553
2562.803	1570.0276	3702.5645	123.5858
3864.825	9.9376	3759.5293	162.1811
3865.9131	103.332	3759.9788	480.2756

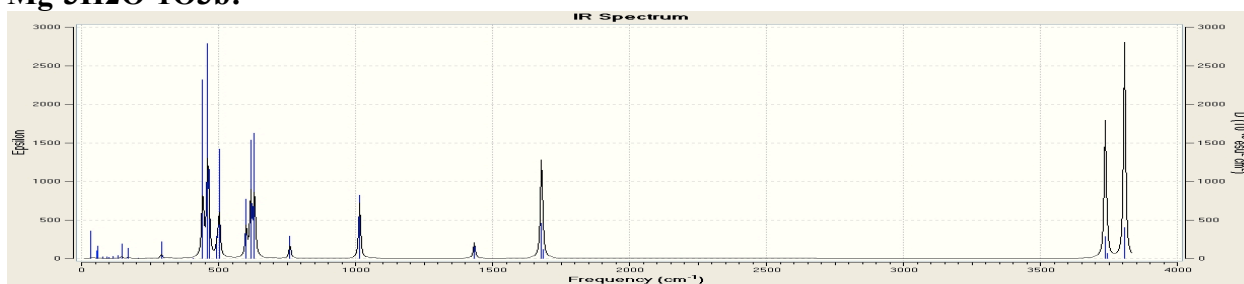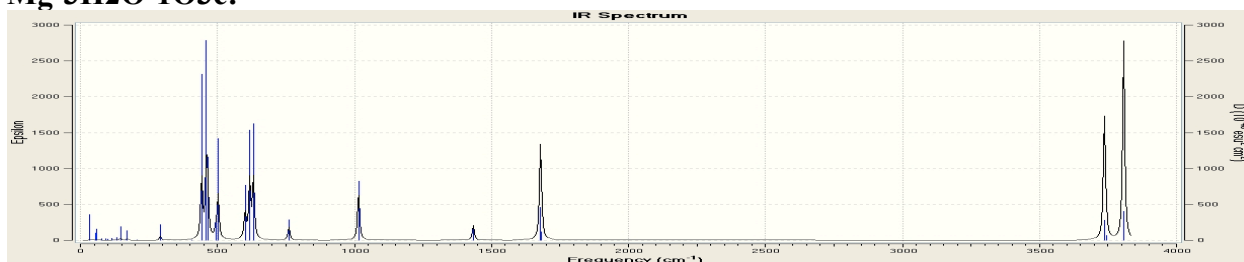**Mg-3H2O-1O3a:**

Mg2-3H2O-1O3b:

Mg-3H2O-1O3b:
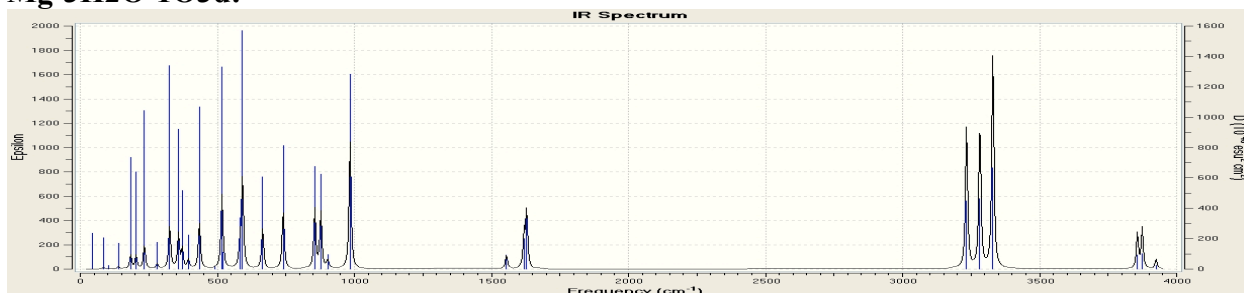

Mg-3H2O-1O3c:

Mg-3H2O-1O3d:

Figure 4. IR intensity as a function of frequency calculated using DFT for Mg-3H2O-1O3a, Mg2-3H2O-1O3b, Mg-3H2O-1O3b, Mg-3H2O-1O3c and Mg-3H2O-1O3d according to frozen phonon approximation.

29

Table 5. Oscillation frequencies and IR intensities for Mg-3H2O-1O3a, Mg2-3H2O-1O3b, Mg-3H2O-1O3b, Mg-3H2O-1O3c and Mg-3H2O-1O3d (see Figure 4).

Mg-3H2O-1O3a		Mg2-3H2O-1O3b	
Freq(1/cm)	Inten(KM/Mol)	Freq(1/cm)	Inten(KM/Mol)
32.2105	0.1975	33.6717	3.0131
50.6136	0.8088	54.6508	1.4046
60.5462	1.9592	58.5217	2.3405
79.7022	1.487	78.329	0.459
95.5167	1.2126	91.6204	0.4795
99.4043	1.0273	99.1427	0.4783
114.3158	1.0111	116.3889	0.801
127.5627	1.0339	134.1213	1.2543
137.4292	1.218	147.6397	7.1116
210.9399	0.4252	169.9682	5.775
247.2768	8.0046	206.7095	0.3201
304.0167	14.36	291.8604	16.0407
407.6182	0.1916	408.2346	0.4106
450.392	285.0747	442.4516	257.0734
462.5326	214.0928	459.8073	321.1585
469.6819	219.217	464.8418	134.9852
496.7593	32.7997	493.7506	36.2967
503.5761	150.4249	502.4948	178.9105
605.198	135.4365	600.9844	115.9111
621.661	253.7853	617.8451	237.858
629.6363	180.0215	631.2166	257.2508
748.3948	22.18	760.9648	55.0591
1107.076	193.9602	1015.0628	209.6179
1382.3593	61.0911	1433.8429	60.9739
1678.6802	200.011	1678.3737	180.573
1679.4196	185.299	1679.0385	193.9314
1683.644	45.897	1683.45	49.9644
3732.7842	264.6268	3736.3147	264.7338
3733.4141	255.6245	3736.7974	242.5301
3739.9951	55.8343	3743.2419	62.5816
3802.157	205.1674	3806.251	225.0797
3803.6045	353.3185	3807.1108	228.1155
3803.7693	275.225	3808.1206	386.2985

Table 5 (continued).

| Mg-3H2O-1O3b		Mg-3H2O-1O3c		Mg-3H2O-1O3d	
Freq(1/cm)	Inten(KM/Mol)	Freq(1/cm)	Inten(KM/Mol)	Freq(1/cm)	Inten(KM/Mol)
44.998	2.6555	33.6727	3.0123	44.9949	2.6552
85.3087	4.388	54.6509	1.4042	85.3052	4.3881
101.786	0.6331	58.5234	2.3413	101.7847	0.6328
140.1145	5.9725	78.33	0.4591	140.1148	5.9725
183.8086	33.9426	91.6203	0.4796	183.8039	33.9403
203.4445	32.5838	99.1422	0.4782	203.444	32.5859
233.9824	61.1673	116.3873	0.8011	233.9811	61.1661
280.5918	12.4785	134.1211	1.254	280.5868	12.4797
325.9727	109.5987	147.6383	7.112	325.9727	109.595
358.3042	82.7844	169.9678	5.7751	358.3026	82.7855
372.0196	48.3025	206.7093	0.32	372.0202	48.3036
394.5096	22.3016	291.8601	16.0406	394.51	22.3029
434.3322	116.2276	408.2351	0.4105	434.3313	116.2295
489.0051	1.9227	442.4522	257.075	489.0057	1.923
516.5334	172.1702	459.8065	321.1473	516.5338	172.1853
521.9176	14.6265	464.8412	134.9906	521.9169	14.6072
582.3173	49.3246	493.7512	36.3022	582.316	49.3328
591.7488	233.1108	502.4935	178.9076	591.7491	233.1038
665.2133	101.4021	600.9845	115.9166	665.2123	101.3977
740.2394	150.8395	617.845	237.8661	740.2379	150.8437
855.519	144.6909	631.2164	257.2394	855.5229	144.7149
877.5847	137.6733	760.9651	55.0586	877.5851	137.6606
902.469	21.6337	1015.063	209.6178	902.4697	21.6344
984.3825	316.3369	1433.844	60.974	984.3844	316.3306
1554.9099	35.9722	1678.374	180.5711	1554.9062	35.971
1619.2921	81.3122	1679.039	193.9305	1619.2913	81.3131
1628.5105	141.8342	1683.45	49.9676	1628.5096	141.8328
3233.6333	363.5954	3736.315	264.7302	3233.6299	363.6014
3282.2258	380.9612	3736.797	242.535	3282.2307	380.925
3329.6975	556.6352	3743.242	62.5798	3329.6943	556.6632
3857.0508	88.5886	3806.251	225.0645	3857.052	88.589
3874.4756	97.3466	3807.111	228.1334	3874.4753	97.3467
3925.0054	24.6117	3808.121	386.2956	3925.0049	24.6115

Mg-5H2O-1O3c:
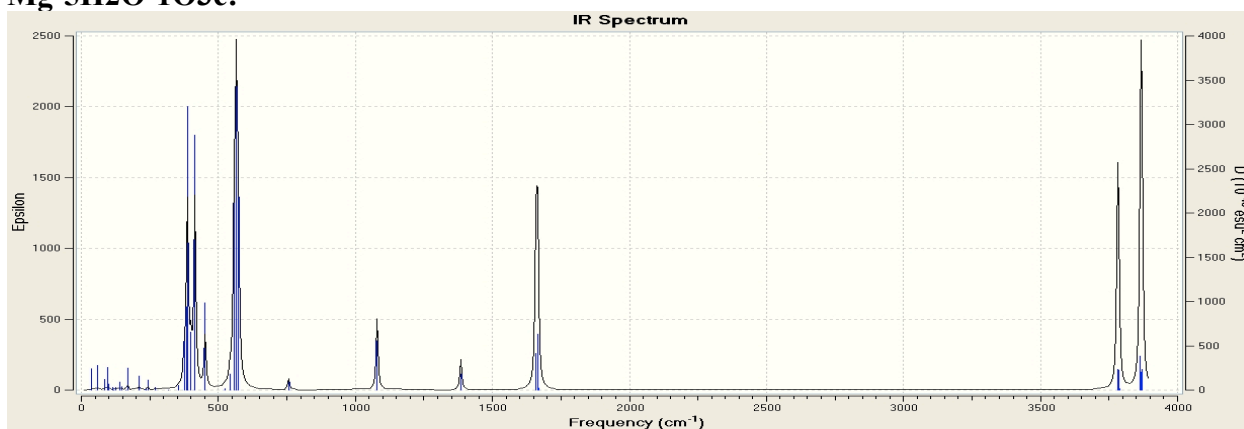
Figure 5. IR intensity as a function of frequency calculated using DFT for Mg-5H2O-1O3c according to frozen phonon approximation.

Table 6. Oscillation frequencies and IR intensities for Mg-5H2O-1O3c (see Figure 5).
**Mg-5H2O-1O3c**

Freq(1/cm)	Inten(KM/Mol)	Freq(1/cm)	Inten(KM/Mol)
35.1688	2.1297	415.1529	93.5103
57.4934	0.2562	451.5817	111.7319
58.0137	3.9986	525.4435	2.0861
85.9678	2.5991	542.3883	24.8932
94.6081	6.1453	557.9902	362.8925
99.8833	1.7197	565.4966	560.2988
112.985	0.8802	572.7684	343.0399
117.429	0.0007	756.3032	24.2266
124.6666	0.9448	1079.2524	150.4035
140.7385	3.2001	1384.7188	62.9591
149.2038	1.3027	1658.066	132.5163
161.3987	0.0251	1659.5944	172.0498
168.3744	10.3494	1664.5553	78.8608
210.9177	8.5273	1665.0923	263.0923
236.166	0.3491	1668.4019	10.2169
242.645	6.632	3780.4014	27.3361
268.0628	2.0955	3780.9431	222.0036
269.6426	0.1419	3782.0198	82.2393
317.5786	0.1382	3784.8257	216.5979
355.902	4.6501	3788.3618	17.0396
374.9799	60.0273	3864.3662	0.8856
385.2434	90.4991	3864.823	371.8035
387.3529	311.1549	3868.0459	194.1079
397.4338	15.5245	3868.6863	145.1753
400.0955	65.6664	3870.6726	222.5865
413.7709	298.3269		

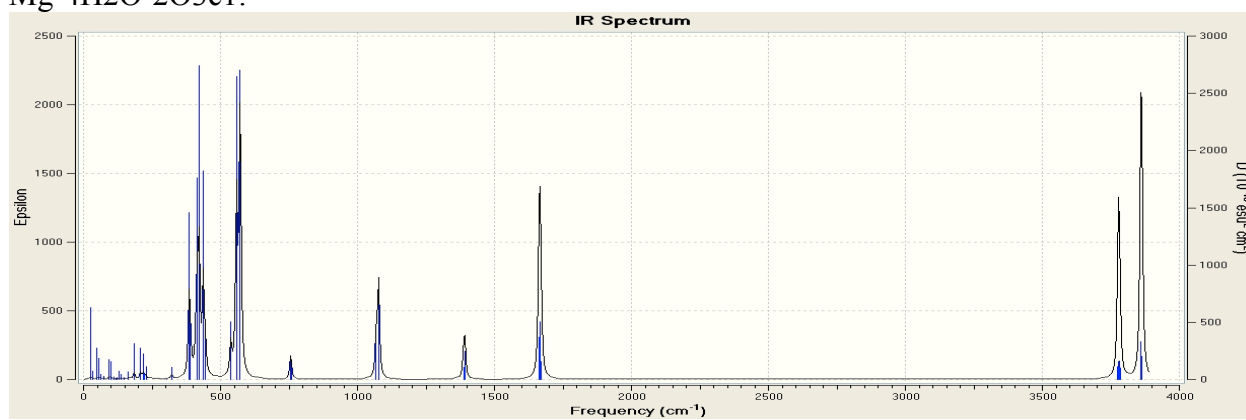Mg-4H2O-2O3b1:
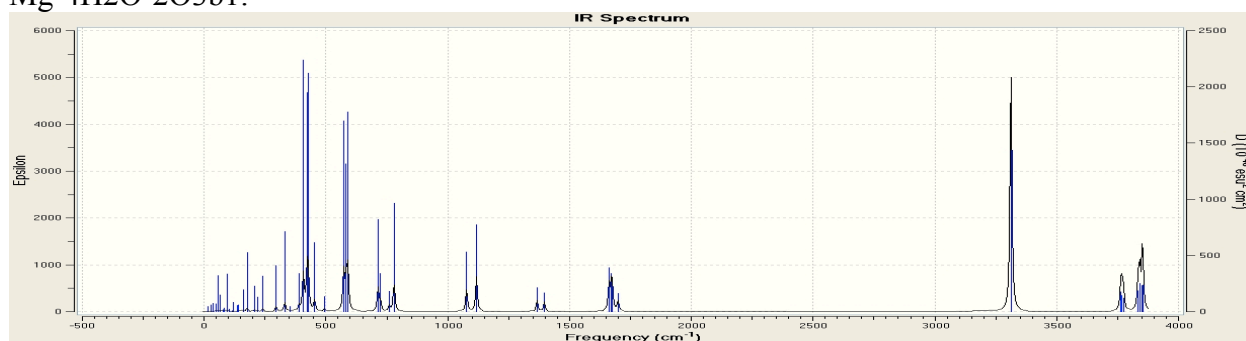
Mg2-4H2O-2O3c1:
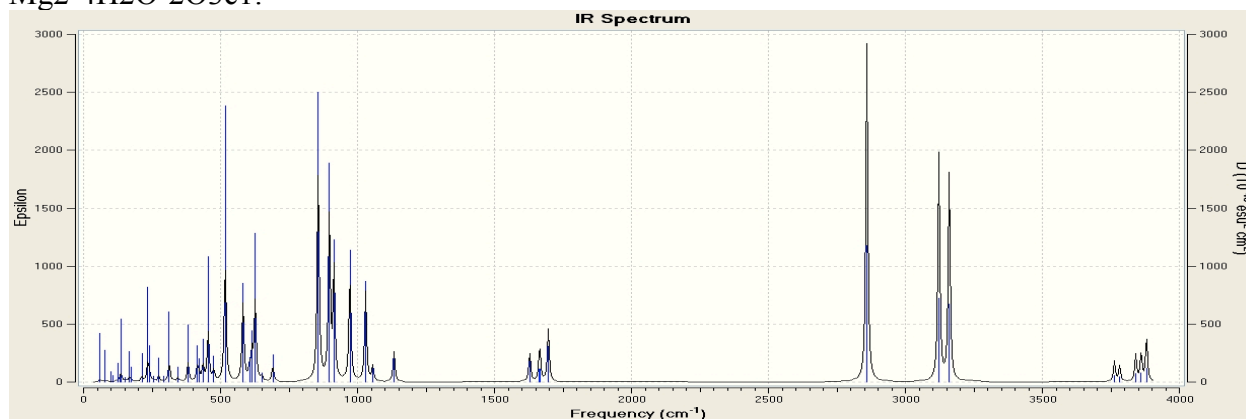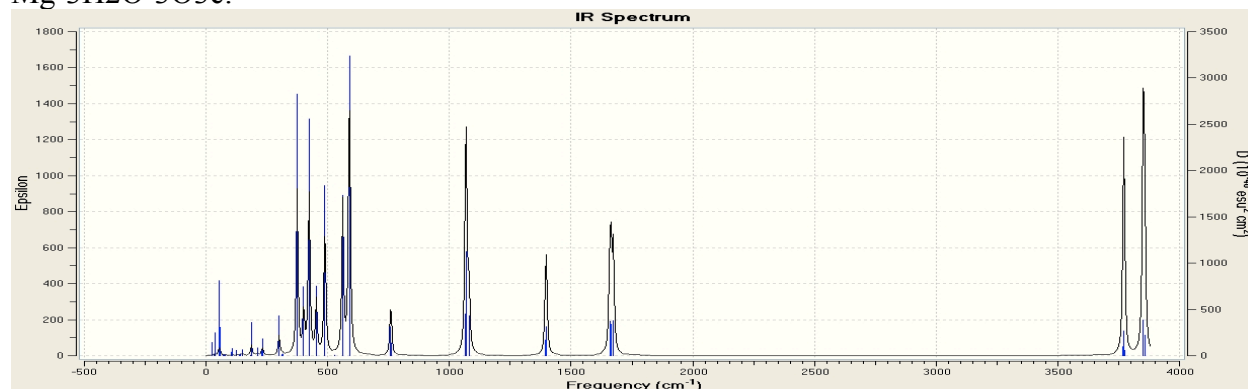

Mg-4H2O-2O3c1:

Figure 6. IR intensity as a function of frequency calculated using DFT for Mg-4H2O-2O3b1, Mg2-4H2O-2O3c1 and Mg-4H2O-2O3c1 according to frozen phonon approximation.

Table 7. Oscillation frequencies and IR intensities for Mg-4H2O-2O3b1, Mg2-4H2O-2O3c1 and Mg-4H2O-2O3c1 (see Figure 6).

Mg-4H2O-2O3b1:   **Mg2-4H2O-2O3c1:**   **Mg-4H2O-2O3c1:**

Freq(1/cm)	Inten(KM/Mol)	Freq(1/cm)	Inten(KM/Mol)	Freq(1/cm)	Inten(KM/Mol)
17.5546	0.1979	61.0974	6.4175	26.7704	4.202
27.4616	0.4132	75.9989	5.2821	33.4182	0.6329
37.7744	0.7	100.5953	2.2052	46.5373	3.1761
50.2451	0.9014	106.1246	1.4702	54.9549	2.527
56.264	4.5697	126.4517	5.1006	62.2253	0.6741
66.6351	2.4813	133.4308	2.2744	72.3367	0.4961
76.587	0.3477	137.881	18.7591	91.485	4.0302
80.6774	0.6389	152.5699	1.5998	99.585	3.8642
95.4932	7.9847	167.1704	11.0785	109.8884	0.604
102.2573	0.6354	173.7561	5.6946	119.8486	0.27
115.3309	0.2387	213.2897	13.0628	121.3485	0.4595
118.7343	2.4543	234.415	48.1811	131.464	2.4453
136.6456	1.8635	240.5457	18.9392	138.0665	1.4676
140.1505	2.0935	257.0184	3.4116	148.4179	0.6254
160.2528	7.8791	274.2545	14.3076	161.2825	2.7313
176.1705	23.324	292.2655	3.7322	184.6454	14.4556
206.3825	11.7542	312.9125	47.6057	207.9481	14.3143
218.3529	7.0271	343.9081	11.0083	218.183	12.115
240.0122	18.9432	381.5567	47.0478	223.1649	2.9551
295.1344	30.2464	414.817	32.5234	228.7999	6.5563
330.9589	59.1243	420.8241	21.5153	305.3751	0.0813
351.5273	4.1384	435.9781	40.3102	322.0235	8.5591
389.4497	33.1134	454.9891	123.1683	385.1486	140.6143
406.8555	228.4286	475.2712	26.8919	386.5691	23.6393
422.2063	206.5776	517.1516	308.8377	390.167	50.4354
426.5248	227.125	581.5585	124.0827	413.3705	182.4903
453.2164	70.1557	582.8933	76.8336	421.2017	289.2989
494.7359	16.8329	605.7295	32.0351	436.6875	199.5979
572.6514	243.6503	615.0644	68.0155	444.4116	54.9945
582.4582	192.2378	626.6294	201.8712	537.629	68.2001
589.4331	262.4468	650.4496	12.3531	558.5453	370.7958
713.7673	146.8864	690.9427	40.5331	570.1666	220.6961
723.6553	61.7879	856.465	537.4037	572.1578	387.7589
759.6468	34.6624	897.172	425.1042	755.4188	34.6475
779.3897	188.6524	914.1653	280.8526	757.7241	20.2728

Mg-4H2O-2O3b1:   **Mg2-4H2O-2O3c1:**   **Mg-4H2O-2O3c1:**

Freq(1/cm)	Inten(KM/Mol)	Freq(1/cm)	Inten(KM/Mol)	Freq(1/cm)	Inten(KM/Mol)
1077.3947	143.5487	972.4461	277.1828	1068.4456	93.4501
1117.9648	216.7688	1029.599	224.814	1077.087	206.3306
1366.7216	73.4907	1055.694	37.2676	1387.1108	36.9235
1396.4812	58.7302	1133.439	75.2458	1391.5997	85.1838
1661.9503	163.8043	1628.777	73.5419	1662.8	154.6684
1671.2581	142.6418	1664.569	46.7606	1664.4594	116.9319
1675.6841	122.6543	1665.715	46.1215	1666.8083	209.9494
1699.1356	68.8798	1696.522	131.1133	1671.2275	64.9708
3312.3059	1642.366	2859.248	844.8166	3775.5078	106.1763
3763.6101	166.2732	3122.17	567.7547	3777.9807	150.0467
3768.927	136.1429	3159.888	530.7626	3779.8474	152.1234
3774.3518	113.1469	3763.096	50.7964	3783.3606	93.19
3834.3547	179.4872	3782.247	39.9671	3858.9082	184.3879
3840.7473	241.7699	3840.754	67.7366	3860.2549	77.9109
3851.8357	227.1241	3860.605	73.7528	3861.0564	320.2449
3852.5171	229.4043	3880.228	114.4645	3863.9939	193.5062

Mg2-3H2O-3O3c:
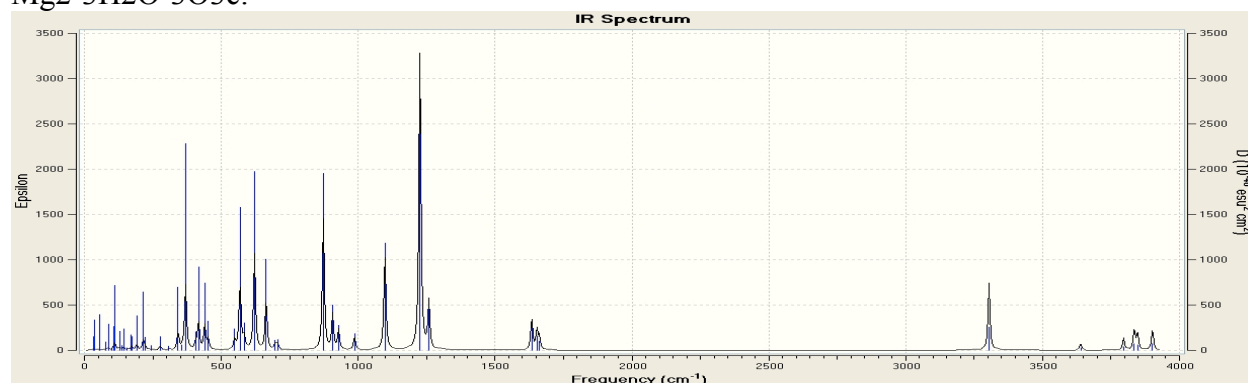
Mg-3H2O-3O3c:

Figure 7. IR intensity as a function of frequency calculated using DFT for Mg2-3H2O-3O3c and Mg-3H2O-3O3c according to frozen phonon approximation.

Table 8. Oscillation frequencies and IR intensities for Mg2-3H2O-3O3c and Mg-3H2O-3O3c (see Figure 7).

Mg2-3H2O-3O3c: **Mg-3H2O-3O3c:**

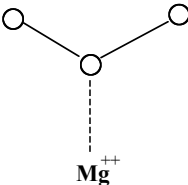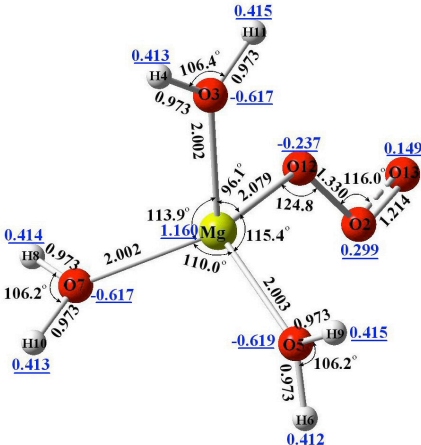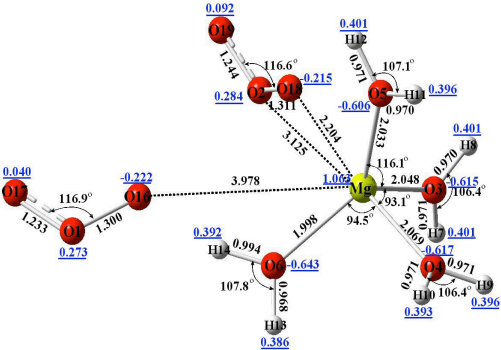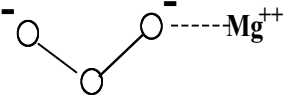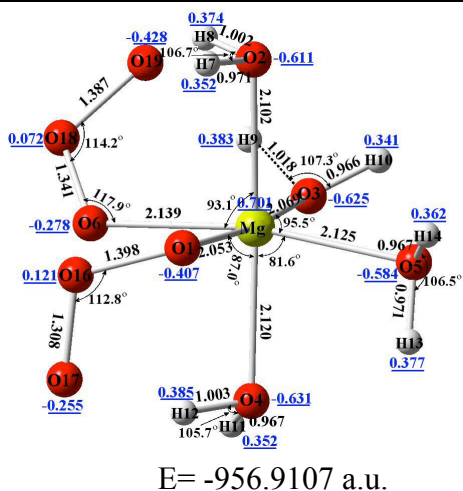| Freq(1/cm)	Inten(KM/Mol)	Freq(1/cm)	Inten(KM/Mol)
31.8508	1.216	23.637	0.865
36.8884	3.0813	33.7162	0.1406
56.1684	5.5407	36.8805	0.0547
78.2525	1.849	38.4224	2.3861
89.0286	6.389	53.2791	10.8443
99.6524	0.6926	59.354	4.5723
107.9021	7.1925	72.2505	0.1579
111.4316	19.9782	72.563	0.2811
129.093	6.7843	78.0343	0.2745
138.7237	1.8738	104.5382	1.052
144.2633	8.5637	108.9378	2.0904
155.2794	0.9475	122.8486	0.3834
171.7218	7.5036	122.9668	1.83
174.9691	6.524	138.5834	0.1421
190.7173	18.0937	141.4143	0.3627
214.9856	34.627	149.1933	2.3841
222.3625	7.9359	149.9124	0.0074
245.4183	3.08	181.0995	0.3959
276.243	2.1074	186.6644	16.8935
277.7571	10.3962	209.8573	4.6218
307.3403	3.3372	229.3121	3.0761
342.0606	59.7588	231.9647	10.6348
356.8069	5.3626	299.7523	32.4523
369.5571	211.3072	311.5036	0.9567
406.2315	20.9872	317.7048	1.3736
416.7749	95.93	374.1807	264.8275
439.4549	81.9049	400.8757	75.0856
452.4302	36.4882	423.2185	271.171
548.5284	32.4117	453.0244	85.17
568.2863	225.003	488.3726	225.1318
583.3098	44.5627	528.7114	0.5651
621.3742	307.8566	561.3878	243.9477
663.8044	167.1951	588.7456	478.256

Table 8 (continued).

Mg2-3H2O-3O3c: **Mg-3H2O-3O3c:**

Freq(1/cm)	Inten(KM/Mol)	Freq(1/cm)	Inten(KM/Mol)
697.231	19.9713	758.358	5.7964
705.6361	21.3551	758.969	60.1038
872.6838	427.6228	759.5663	25.6726
906.682	113.4851	1066.0992	120.3852
928.3463	64.3229	1068.3141	301.9677
986.7503	45.0213	1080.0426	116.9579
1097.7449	325.142	1394.1597	59.2762
1225.6478	990.6257	1397.9274	111.0889
1258.3022	153.8299	1400.0411	27.9875
1634.0455	107.3306	1658.9528	154.6378
1652.8894	65.5759	1665.3375	142.8381
1661.821	41.5298	1673.7437	158.4617
3304.3079	214.1861	3768.7122	94.2957
3639.4629	23.0007	3771.623	252.1519
3795.717	39.7622	3774.2883	53.4047
3835.0083	70.0881	3849.4319	50.2663
3846.8594	56.6673	3851.6162	372.0955
3901.6206	71.8987	3857.1069	212.6177

Mg2-2H2O-4O3c:
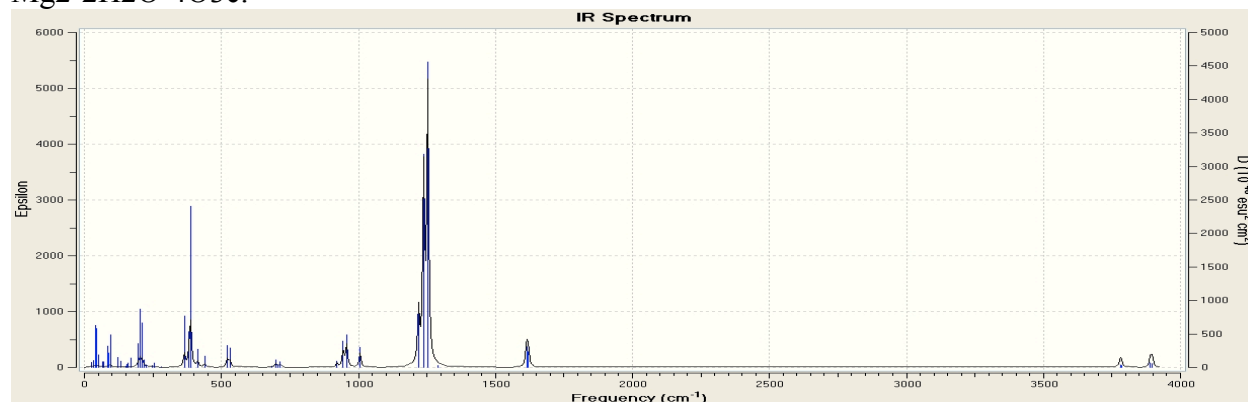
Mg2-1H2O-5O3c:
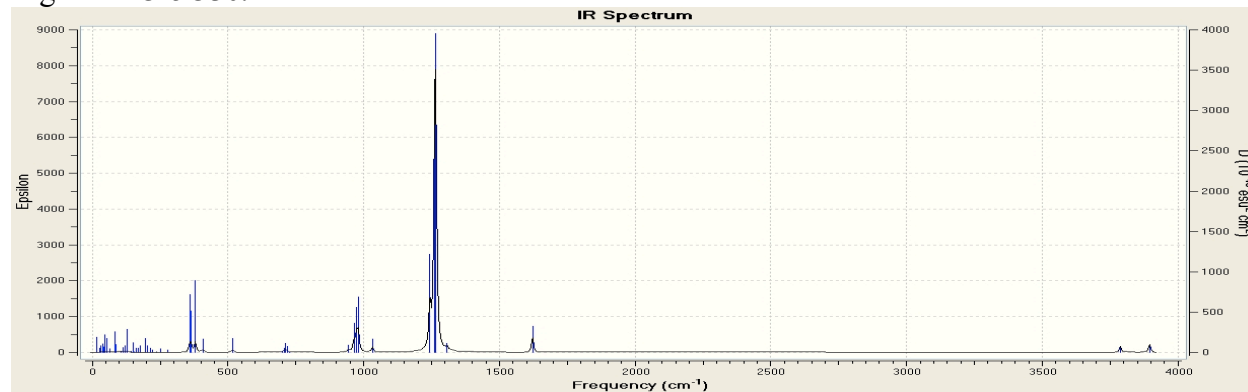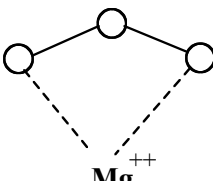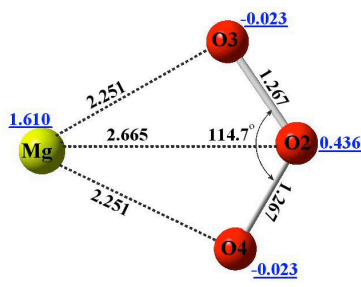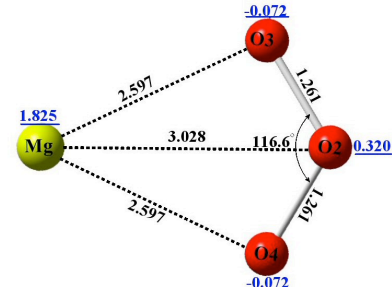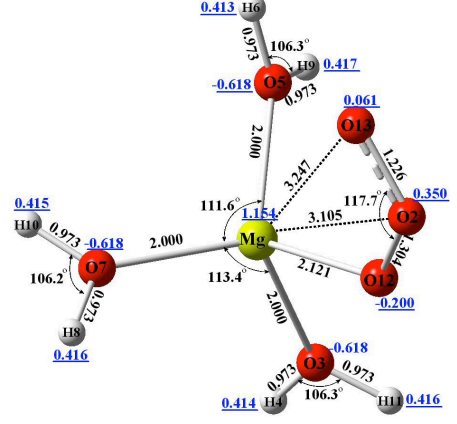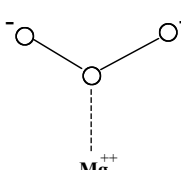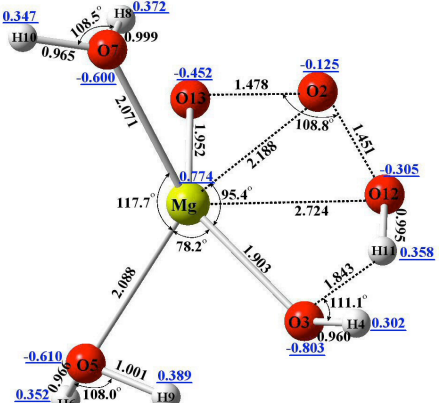
Figure 8. IR intensity as a function of frequency calculated using DFT for Mg2-2H2O-4O3c and Mg2-1H2O-5O3c according to frozen phonon approximation.

Table 9. Oscillation frequencies and IR intensities for Mg2-2H2O-4O3c and Mg2-1H2O-5O3c (see Figure 8).

Mg2-2H2O-4O3c		Mg2-1H2O-5O3c:	
Freq(1/cm)	Inten(KM/Mol)	Freq(1/cm)	Inten(KM/Mol)
25.4758	0.4667	17.1277	0.8016
33.8072	0.8871	28.7471	0.3679
39.8152	6.2237	30.4322	0.6209
45.8549	6.7147	37.8103	0.9723
52.4466	2.405	42.7413	0.7424
65.5507	1.4426	46.4552	2.5241
68.8647	1.4492	52.1435	2.249
83.5864	6.6789	63.0421	0.7503
88.8999	4.7029	82.3441	5.3251
96.3906	11.6657	88.1793	2.2144
122.2098	4.6092	107.1708	0.3991
131.9404	2.955	114.0162	1.7652
134.6036	0.7453	119.446	2.4903
151.1244	0.5732	128.5781	9.2383
156.6152	1.774	141.7998	0.5872
159.038	2.4381	151.6614	4.6978
171.1642	6.0388	154.8385	0.1974
197.008	17.6659	160.323	2.2392
202.8882	44.3506	167.8502	2.2559
210.7264	35.0457	177.0788	3.6108
217.7264	6.2532	195.4187	1.9448
226.5953	2.1558	196.13	8.6072
247.1795	1.9772	204.4497	4.4115
255.9211	4.2166	214.4763	2.6726
279.4199	0.5235	223.5	1.7967
303.0733	0.0369	238.0028	0.5756
365.1768	70.0195	252.7878	2.7722
382.1308	50.8448	278.0061	2.1244
387.6772	233.7623	359.5885	64.6593
413.5882	28.4378	364.0351	47.1386
438.8284	18.1932	379.6389	85.274
521.6522	43.311	408.2349	16.8874
531.0671	38.1732	516.1767	22.933
685.6868	1.85	701.6434	0.9213
698.2902	18.9648	707.7837	9.4715
706.7123	6.7232	712.9189	19.7599
714.4663	14.3761	718.1377	14.1011
922.1485	21.8475	725.3958	1.3881
944.3974	92.2665	944.2793	20.9056
957.0295	116.276	963.8673	88.2924
1006.13	76.0001	973.3368	137.2337
1219.459	274.9522	979.8931	169.6827
1238.046	989.2746	1032.1477	42.8604
1253.02	1431.5426	1243.8636	378.7868
1288.447	9.6345	1261.4062	895.6247
1613.815	126.178	1262.3949	827.8964
1620.344	96.9554	1266.0695	1253.8392
3780.098	38.8964	1307.4706	36.8465
3784.776	29.0075	1622.1887	133.0844
3890.562	62.7445	3787.7356	49.6172
3897.779	52.4055	3895.5608	69.6447

Table 10. Energies, geometries and charges for $Mg^{++} \cdot n(H_2O) \cdot m(O_3)$ with and without a water solvent background after geometry optimization (only for those molecules where stationary points were found).

A	Opt without water solvent	Opt in water solvent
Mg^{++}	2 positive charges in complex	
Mg-1O3a	E= -424.7322 a.u.	E= -425.2642 a.u.
Mg-3H2O-1O3a	E= -654.3201 a.u.	Convergence failure
B	Opt without water solvent	Opt in water solvent
Mg^{++}	No charges in complex	
Mg2-3H2O-1O3b		Convergence failure

	E= -655.0092 a.u.	
Mg++	**2 positive charges in complex**	
Mg-3H2O-1O3b	E= -654.3221 a.u.	Convergence failure .
Mg-4H2O-2O3b1	E= -956.2325 a.u.	Convergence failure
C	**Opt without water solvent**	**Opt in water solvent**
	No charges in complex	

Mg2-4H2O-2O3c1	 E= -956.9107 a.u.	Convergence failure
Mg2-3H2O-3O3c	 E= -1105.8748 a.u.	 E= -1105.8918 a.u.
Mg2-2H2O-4O3c	 E= -1254.8412 a.u.	 E= -1254.8634 a.u.
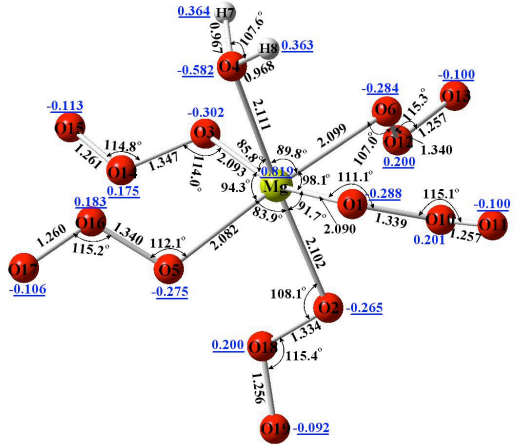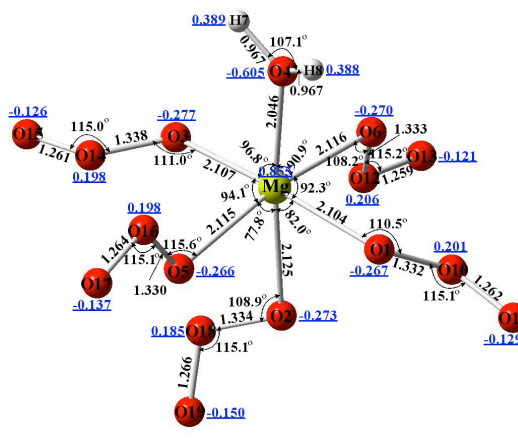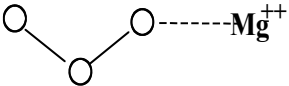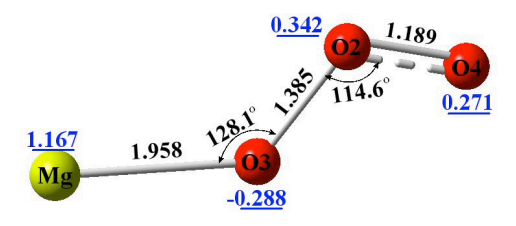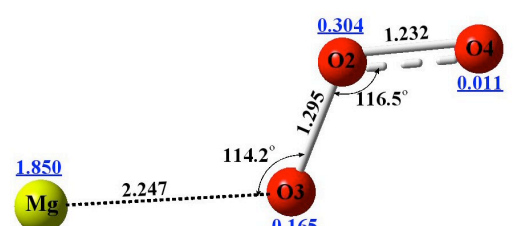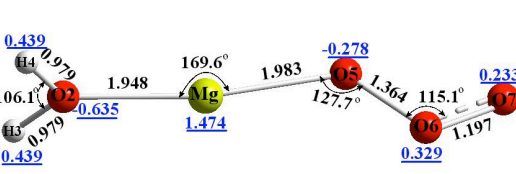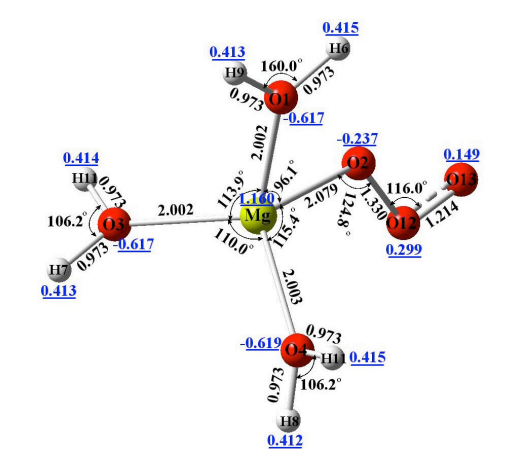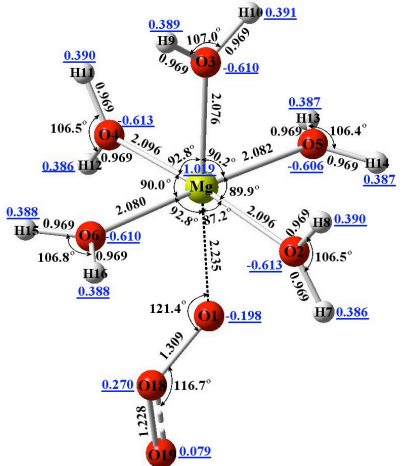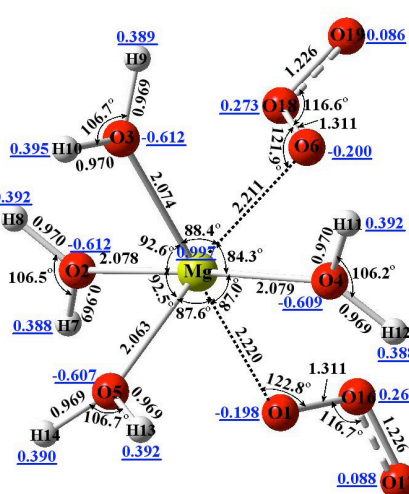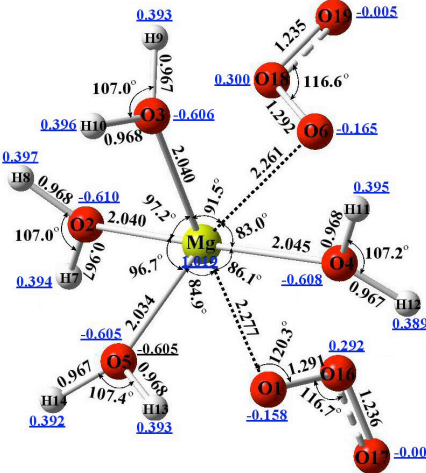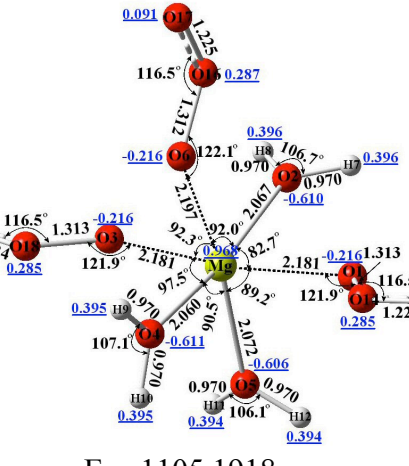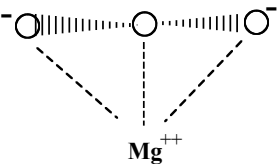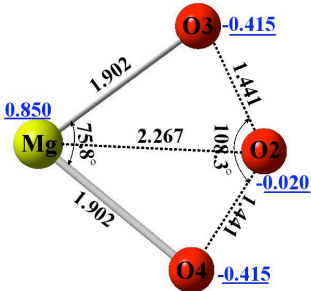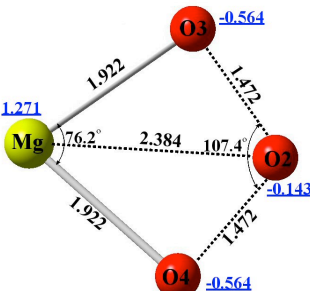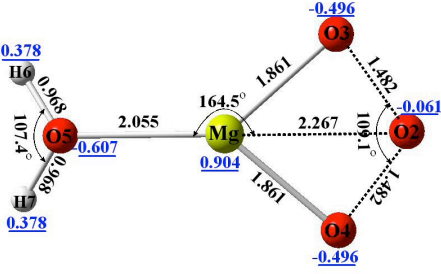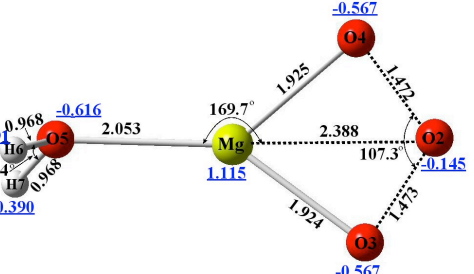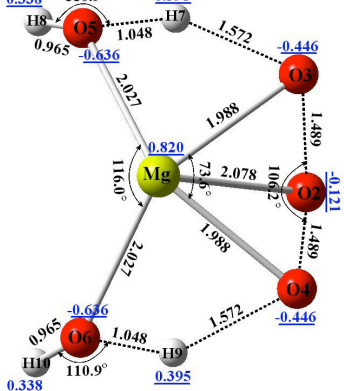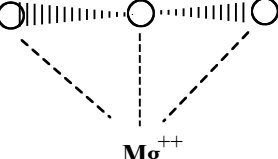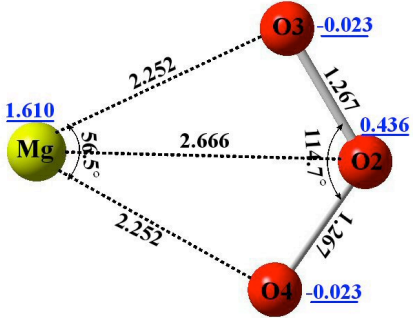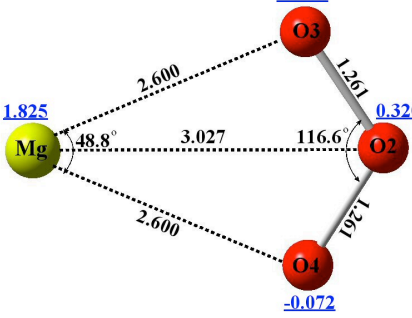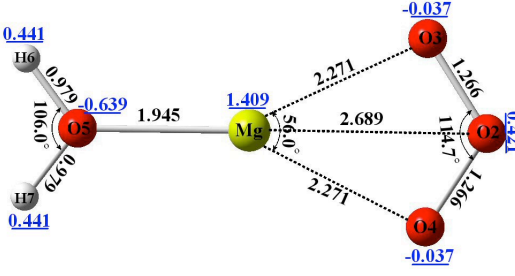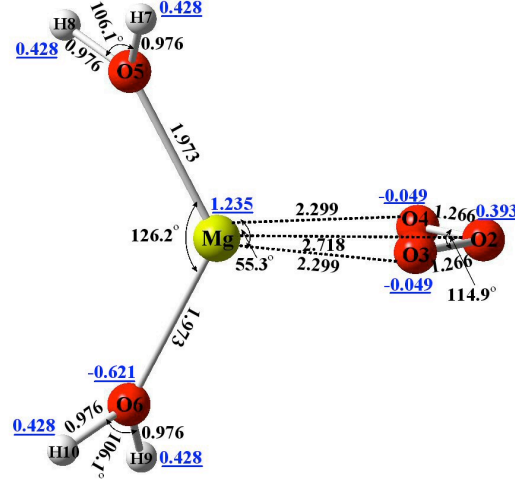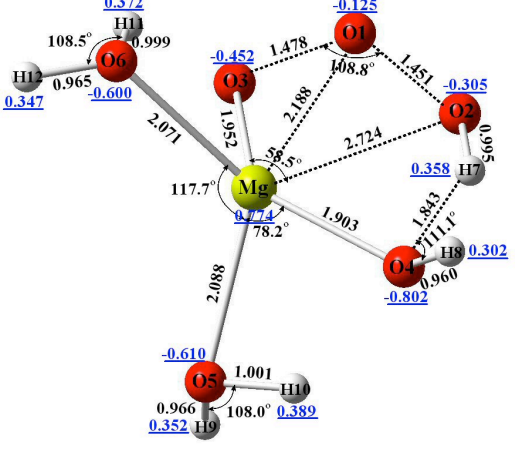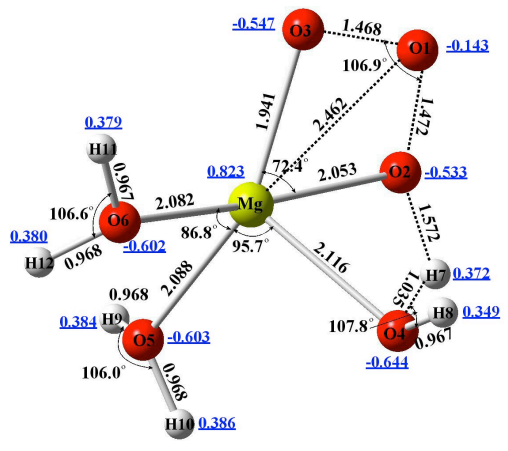
Mg2-1H2O-5O3c	E= -1403.8146 a.u.	E= -1403.8317 a.u.
	2 positive charges in complex	
Mg-1O3c	E= -424.7415 a.u.	E= -425.2680 a.u.
Mg-1H2O-1O3c	E= -501.2889 a.u.	Convergence failure
Mg-3H2O-1O3c	E= -654.3221 a.u.	Convergence failure .

Mg-5H2O-1O3c	E= -807.2784 a.u.	Convergence failure
Mg-4H2O-2O3c1	E= -956.2339 a.u.	E= 956.5133 a.u.
Mg-3H2O-3O3c	E= -1105.1918 a.u.	Convergence failure .
D	**Opt without water solvent**	**Opt in water solvent**

 (d)	**No charges in complex**	
Mg2-1O3d	 E= -425.5847 a.u.	 E= -425.6743 a.u.
Mg2-1H2O-1O3d	 E= -502.05487 a.u.	 E= -502.1302 a.u.
Mg2-2H2O-1O3d	 E= -578.5279 a.u.	Convergence failure
 Mg^{++}	**2 positive charges in complex**	

44

Mg-1O3d	E= -424.7322 a.u.	E= -425.2642 a.u.
Mg-1H2O-1O3d	E= -501.2821 a.u.	Convergence failure
Mg-2H2O-1O3d	E= -577.8103 a.u.	Convergence failure
Mg-3H2O-1O3d	E= -655.0092 a.u.	E= -655.0367 a.u.

Figure 9A. IR intensity as a function of frequency calculated using DFT for Mg-1O3a in water solvent according to frozen phonon approximation.

Figure 9B. IR intensity as a function of frequency calculated using DFT for Mg2-3H2O-3O3c in water solvent according to frozen phonon approximation.
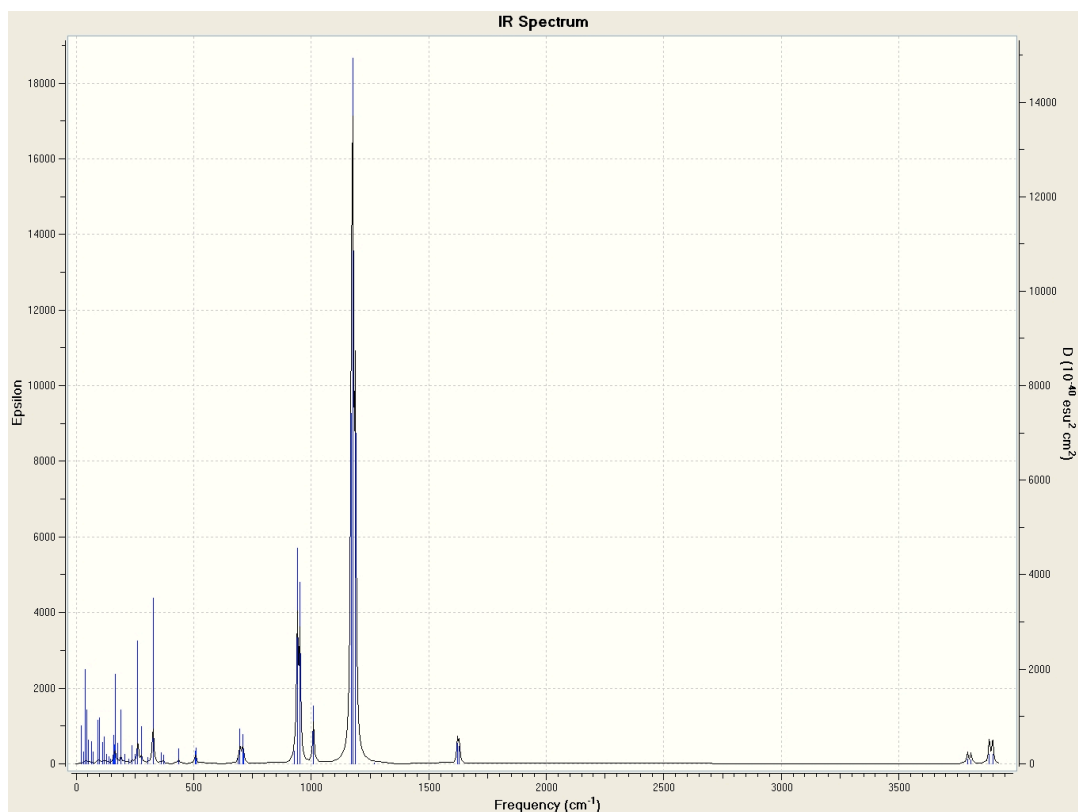
Figure 9C. IR intensity as a function of frequency calculated using DFT for Mg2-2H2O-4O3c in water solvent according to frozen phonon approximation.
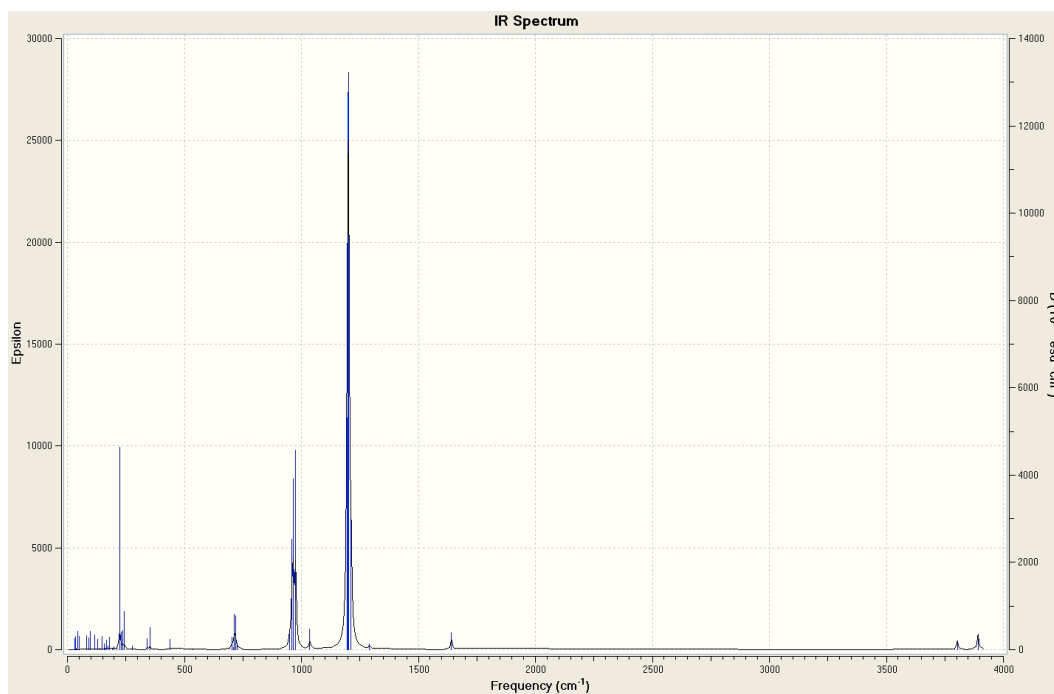
Figure 9D. IR intensity as a function of frequency calculated using DFT for Mg2-1H2O-5O3c in water solvent according to frozen phonon approximation.
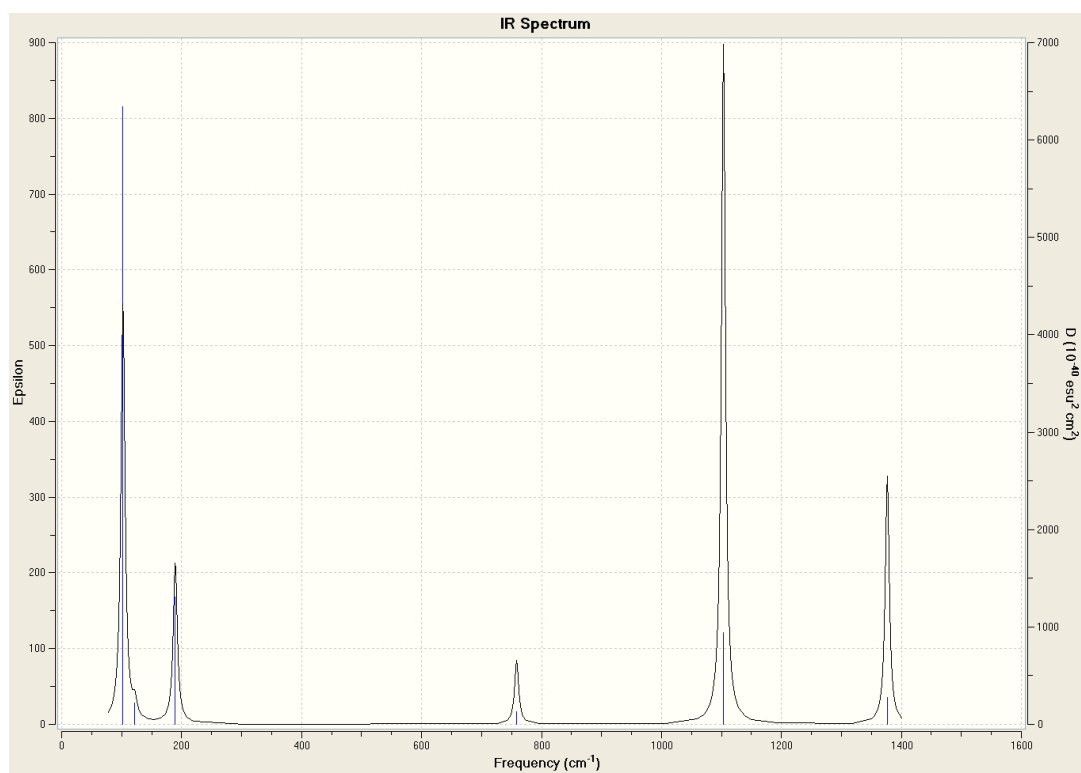
Figure 9E. IR intensity as a function of frequency calculated using DFT for Mg-1O3c in water solvent according to frozen phonon approximation.
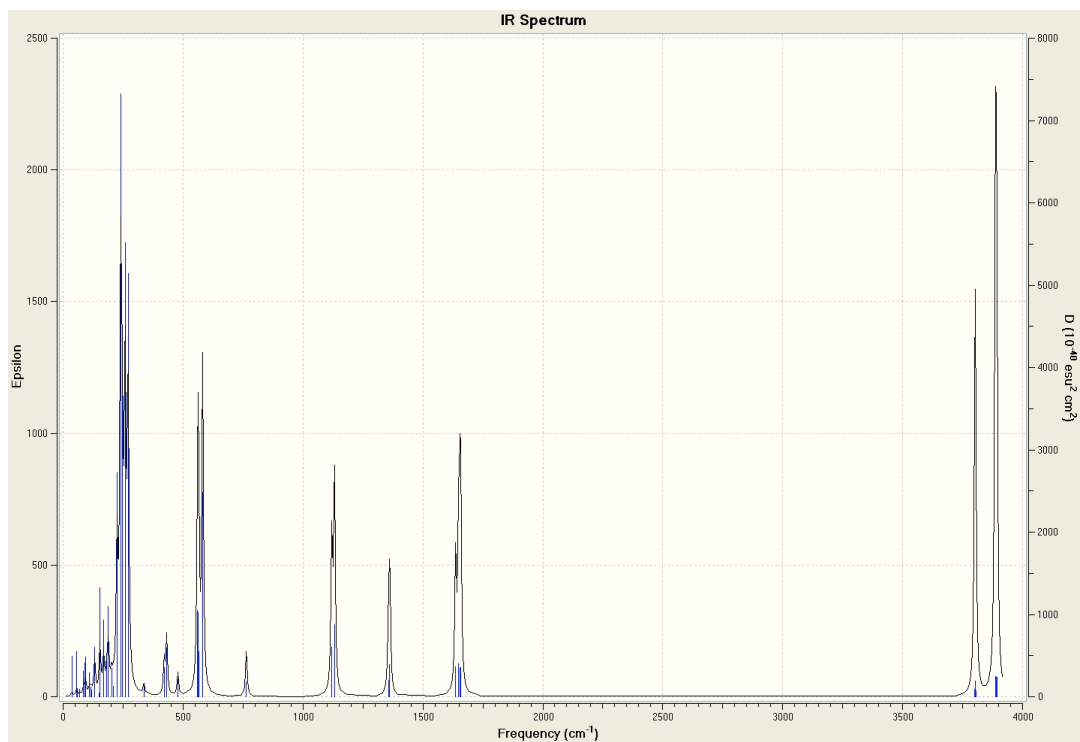
Figure 9F. IR intensity as a function of frequency calculated using DFT for Mg-4H2O-2O3c1 in water solvent according to frozen phonon approximation.
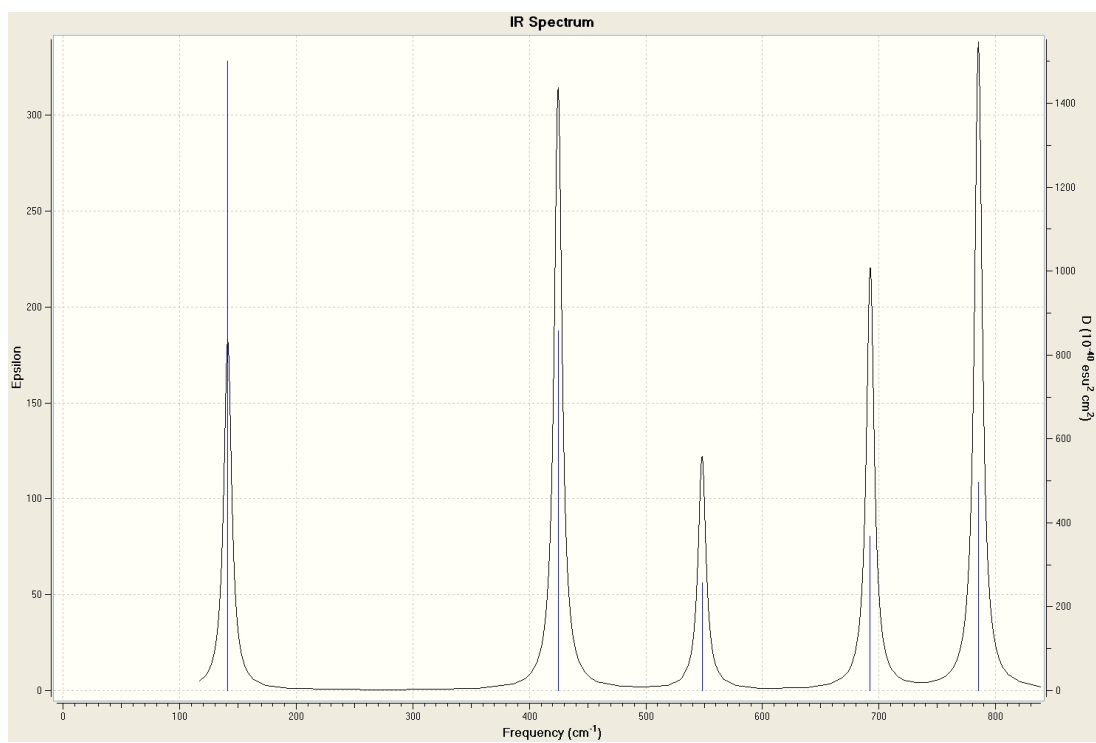
Figure 9G. IR intensity as a function of frequency calculated using DFT for Mg2-1O3d in water solvent according to frozen phonon approximation.

Figure 9H. IR intensity as a function of frequency calculated using DFT for Mg2-1H2O-1O3d in water solvent according to frozen phonon approximation.
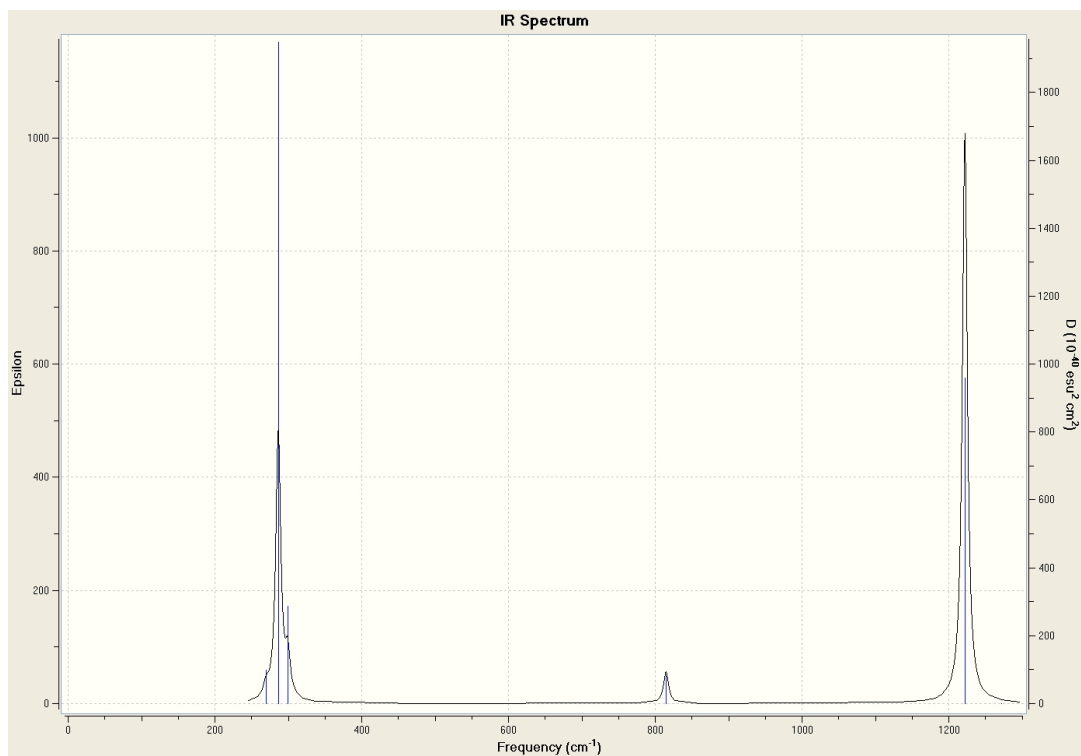

Figure 9I. IR intensity as a function of frequency calculated using DFT for Mg-1O3d in water solvent according to frozen phonon approximation.
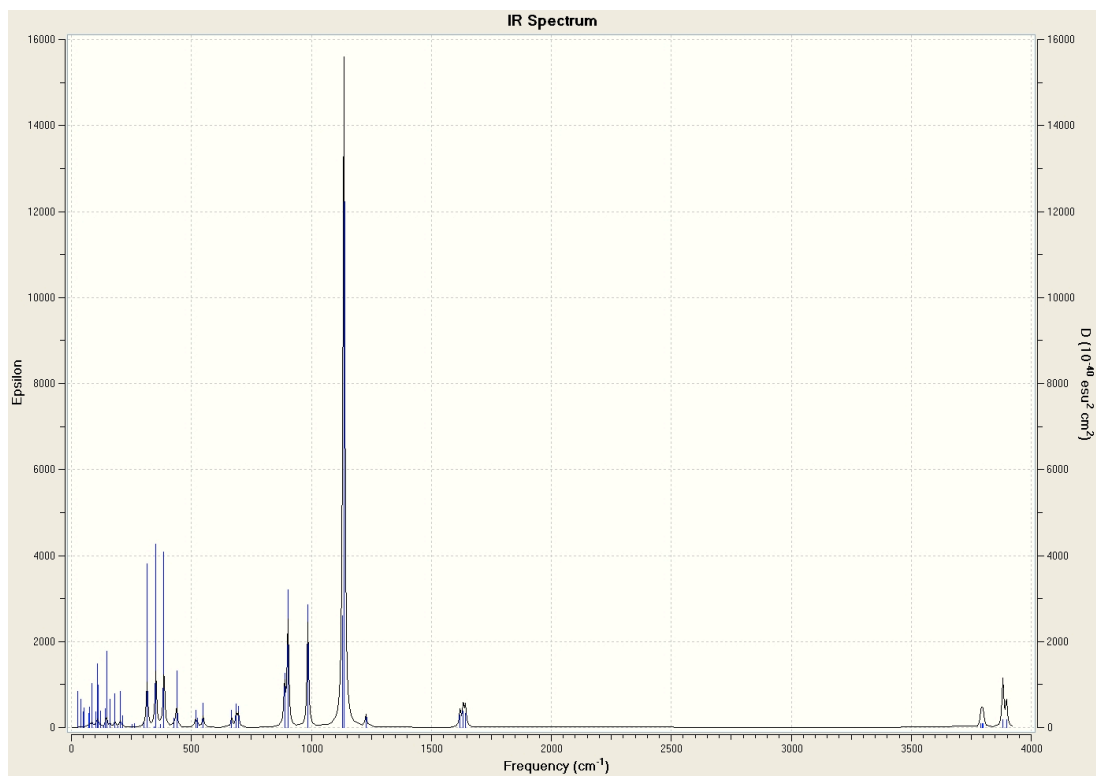
Figure 9J. IR intensity as a function of frequency calculated using DFT for Mg-3H2O-1O2d in water solvent according to frozen phonon approximation.
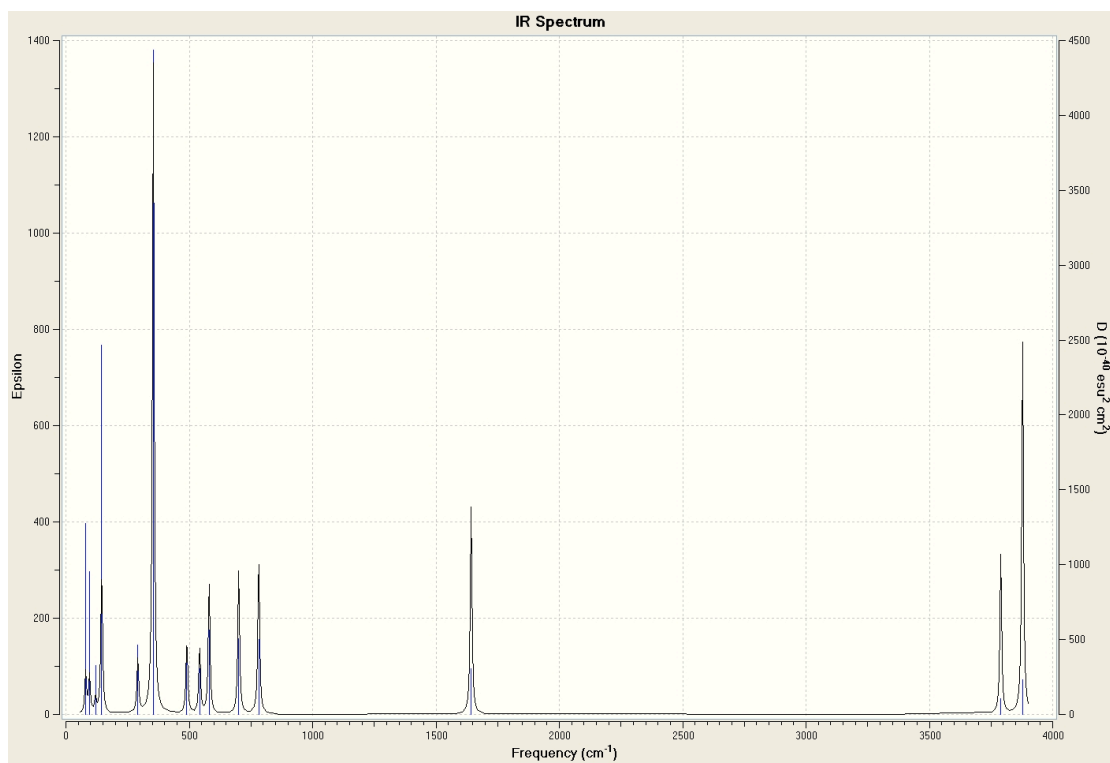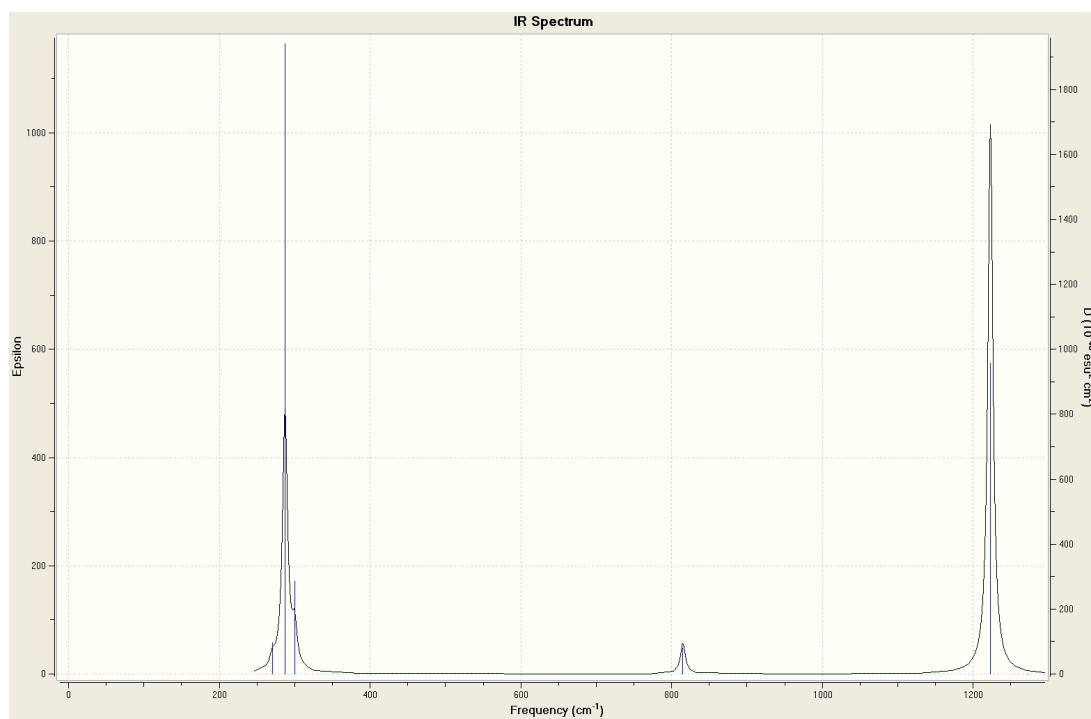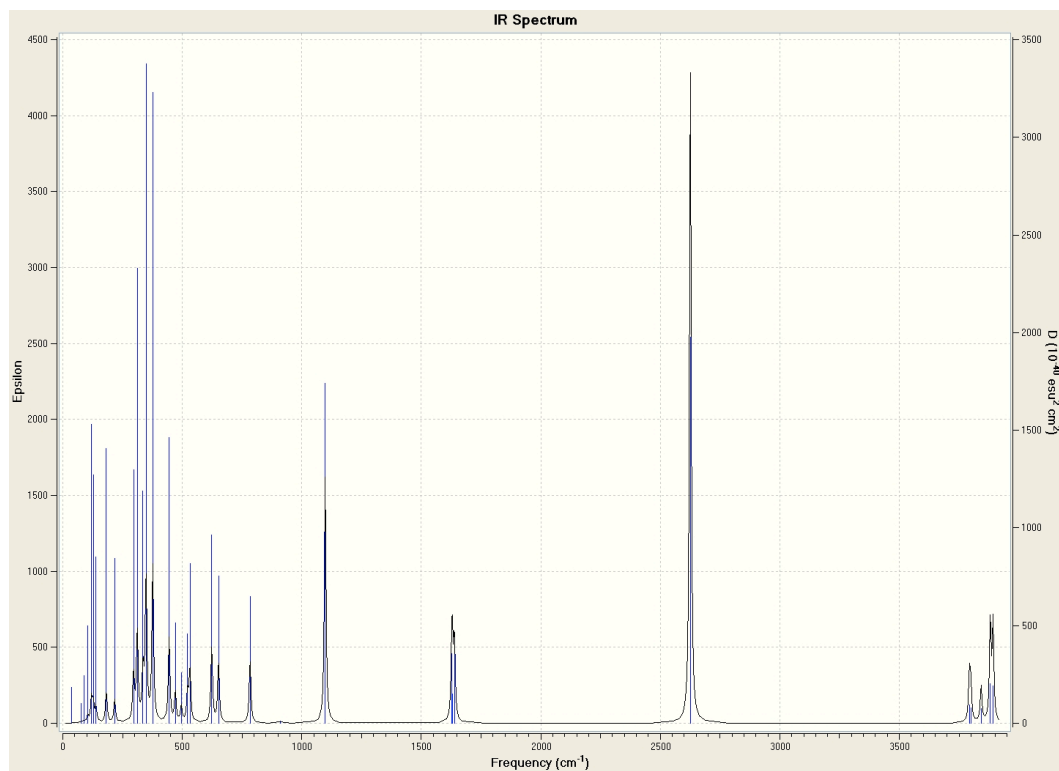
Table 11. IR vibrational frequencies for $Mg^{++} \cdot nH_2O \cdot mO_3$ in water solvent background.

	Mg-1O₃a-water		Mg-1O₃c-water		Mg2-1O₃d-water		Mg-1O₃d-water	
	Freq(1/cm)	Inten(KM/Mol)	Freq(1/cm)	Inten(KM/Mol)	Freq(1/cm)	Inten(KM/Mol)	Freq(1/cm)	Inten(KM/Mol)
1	269.7933	6.5846	102.1686	162.3709	141.1540	53.1105	270.7252	6.5559
2	286.2696	139.7046	122.0137	6.6789	424.6302	91.2653	287.1446	139.7326
3	299.1452	21.5110	189.4085	62.0475	548.1381	35.3507	299.7874	21.5136
4	814.6328	16.3565	758.5497	24.6085	692.4958	63.9607	814.9981	16.3946
5	1221.7743	293.7396	1103.3180	259.8589	785.2272	97.7826	1222.8286	293.6978
6	1272.3048	0.0000	1376.4747	95.1544	903.8866	0.1287	1272.4445	0.0000

Table 12. IR vibrational frequencies for $Mg^{++} \cdot 3H_2O \cdot 3O_3c$ in water solvent background.

Mg2-3H₂O-3O₃c -water

	Freq(1/cm)	Inten(KM/Mol)		Freq(1/cm)	Inten(KM/Mol)
1	26.6890	5.6758	27	371.6356	6.0940
2	38.5272	6.3489	28	385.7418	395.4585
3	48.0644	4.4174	29	427.9078	23.4751
4	52.3838	5.9562	30	438.5391	145.3801
5	72.5051	6.1170	31	517.3337	51.8855
6	75.9618	8.9191	32	524.7413	30.0096
7	85.1248	18.2600	33	549.1138	77.6343
8	86.6142	22.2864	34	668.0539	67.6699
9	100.9011	9.0628	35	687.0217	94.1704
10	107.4554	40.1616	36	696.1097	87.6484
11	112.7013	27.6707	37	888.6460	282.9608
12	123.1408	11.6032	38	902.5340	724.2390
13	134.3007	1.2549	39	985.3349	703.1385
14	142.0157	15.3841	40	1129.9985	738.0101
15	146.8154	65.0550	41	1136.1034	4309.7974
16	162.3411	26.9104	42	1227.8716	81.4878
17	182.0605	36.0079	43	1620.1936	122.2976
18	194.0499	2.1301	44	1633.4756	154.2166
19	203.3028	42.4820	45	1642.4991	133.8621
20	212.9807	14.5693	46	3790.4001	81.9811
21	253.0248	4.5574	47	3795.2258	80.1451
22	263.8419	6.2597	48	3800.8767	90.1716
23	302.9689	9.9626	49	3881.1904	177.0335
24	315.3242	300.3528	50	3883.2961	168.4571
25	343.8841	1.2854	51	3897.0818	185.4820
26	351.7392	375.8502			

Table 13. IR vibrational frequencies for Mg^{++} ·2H$_2$O ·4O$_3$c in water solvent background.

Mg2-2H$_2$O-4O$_3$c -water

	Freq(1/cm)	Inten(KM/Mol)		Freq(1/cm)	Inten(KM/Mol)
1	22.7430	4.5651	27	303.8394	10.3645
2	30.8902	1.9399	28	326.9409	286.9203
3	39.2539	19.6199	29	360.5391	21.0136
4	44.7008	12.7970	30	371.9219	17.6072
5	52.3963	6.4954	31	436.6445	35.0673
6	65.7529	7.7418	32	506.1260	34.2253
7	70.7706	4.3362	33	509.2525	42.5334
8	91.7756	21.2072	34	689.5350	21.9449
9	99.8247	24.2756	35	696.9441	129.2405
10	111.9810	12.6848	36	707.5064	108.4203
11	118.7635	17.1677	37	713.1174	48.9243
12	129.3975	6.3249	38	928.8031	60.6699
13	138.3475	4.9023	39	940.9008	1074.5365
14	144.8882	3.6231	40	951.9070	918.2471
15	157.4191	6.9486	41	1009.1694	310.9560
16	159.5748	23.7659	42	1170.0142	2173.8430
17	164.7342	16.5678	43	1176.4447	4404.2983
18	166.0727	78.5167	44	1187.6586	2554.8877
19	177.6300	19.5221	45	1267.9750	2.6611
20	190.9351	54.8587	46	1622.2017	178.9780
21	205.5630	10.2852	47	1629.7266	151.3179
22	224.3647	5.7176	48	3792.0664	86.2472
23	238.7024	22.7665	49	3806.9580	81.1621
24	249.6144	12.9044	50	3884.8809	191.6571
25	262.3733	170.8705	51	3899.2043	188.6121
26	277.6142	54.2451			

Table 14. IR vibrational frequencies for $Mg^{++} \cdot 1H_2O \cdot 5O_3c$ in water solvent background.

Mg2-1H$_2$O-5O$_3$c -water

	Freq(1/cm)	Inten(KM/Mol)		Freq(1/cm)	Inten(KM/Mol)
1	30.6162	1.9890	27	237.9181	26.3516
2	34.7110	1.4941	28	243.5253	53.9767
3	35.1667	2.6384	29	277.8518	5.8639
4	38.6931	0.3264	30	341.4438	22.3471
5	44.0428	4.7333	31	353.2341	44.8237
6	45.1797	4.3088	32	439.4500	25.6762
7	51.5338	3.8764	33	533.2316	2.9724
8	81.7130	6.6946	34	703.7728	50.1024
9	91.0820	5.9912	35	708.8942	8.0206
10	98.8821	10.4028	36	713.8051	145.2732
11	116.4311	3.2914	37	718.0396	139.0187
12	118.2872	9.9080	38	725.3754	26.2047
13	128.2447	7.3546	39	949.5396	105.8565
14	138.9846	1.2068	40	959.9452	609.9675
15	146.8358	9.1107	41	965.3057	947.6292
16	148.5874	11.2246	42	975.4503	1117.9290
17	157.5461	5.2097	43	1036.2684	122.0387
18	161.9125	1.6745	44	1195.2477	1591.1720
19	166.1588	9.3770	45	1199.3683	3837.1216
20	173.4733	3.6086	46	1202.4399	3987.9131
21	181.2331	12.7681	47	1212.1289	1082.0428
22	193.4466	0.6938	48	1290.9525	41.8872
23	197.1806	3.6843	49	1641.6096	162.5732
24	212.2507	2.7755	50	3803.3777	132.1800
25	223.4802	260.0969	51	3891.7173	234.1042
26	230.4230	22.9002			

Table 15. IR vibrational frequencies for $Mg^{++} \cdot 4H_2O \cdot 2O_3c$ in water solvent background.

Mg-4H₂O-2O₃c -water

	Freq(1/cm)	Inten(KM/Mol)		Freq(1/cm)	Inten(KM/Mol)
1	36.2315	4.5125	27	421.5484	37.8337
2	55.6355	7.684	28	431.8106	64.3138
3	59.3236	1.4515	29	478.5082	25.0524
4	70.2874	1.5403	30	560.9053	147.8506
5	84.4706	6.6115	31	563.3179	143.943
6	90.8587	9.2728	32	565.2202	77.3004
7	95.075	11.5384	33	581.6172	362.511
8	109.9714	7.9375	34	763.7727	34.8877
9	115.5485	3.5226	35	764.307	17.1443
10	119.2872	2.3277	36	1120.0803	169.2501
11	131.0978	19.8303	37	1131.2744	248.8316
12	131.9302	11.5195	38	1356.4987	69.1783
13	132.4804	7.9319	39	1361.9866	133.3774
14	150.6835	1.6006	40	1636.3406	148.9649
15	153.6767	51.0017	41	1648.6666	164.7688
16	168.8817	39.5106	42	1654.8927	142.6954
17	181.595	20.1198	43	1657.7777	149.3898
18	188.4189	51.7318	44	3800.803	89.6875
19	201.8516	17.6168	45	3802.126	139.9209
20	209.7824	6.7327	46	3802.7141	185.1525
21	224.6119	153.1741	47	3804.7615	69.3019
22	239.7355	440.2319	48	3886.2217	244.2535
23	246.3886	243.1599	49	3886.6941	237.5068
24	258.3901	357.1215	50	3891.2029	233.9677
25	270.7921	349.2486	51	3892.3999	234.7578
26	336.9072	11.6585			

Table 16. IR vibrational frequencies for Mg^{++} ·1H2O ·1O3d in water solvent background.

Mg-1H₂O-1O₃d-water
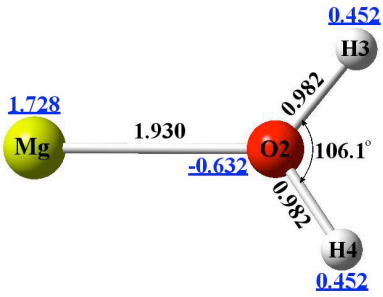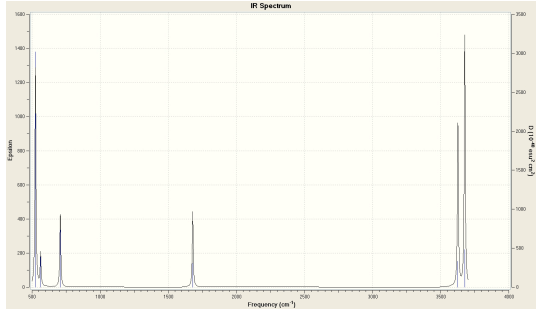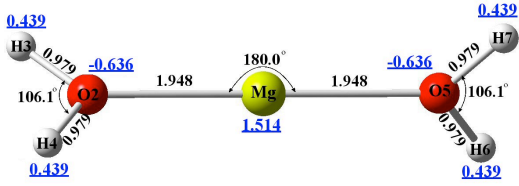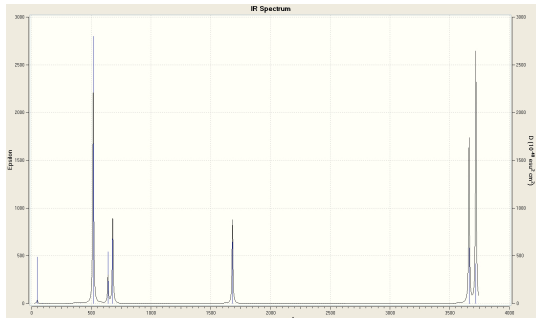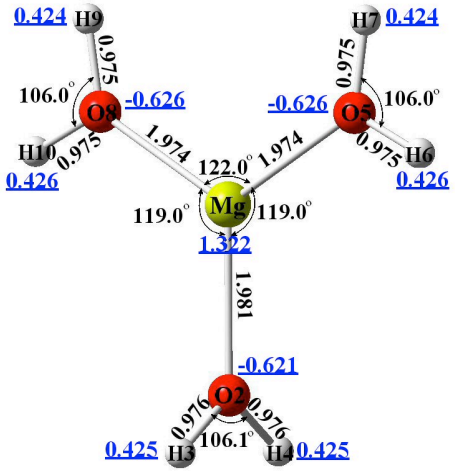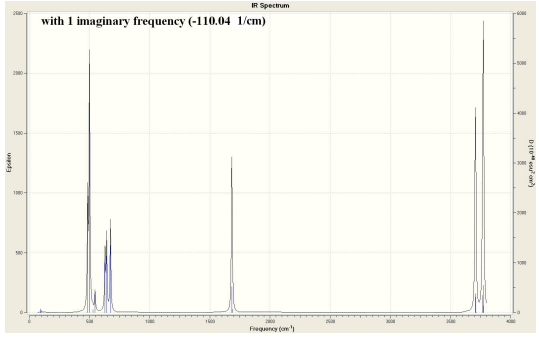
	Freq(1/cm)	Inten(KM/Mol)		Freq(1/cm)	Inten(KM/Mol)
1	80.2864	25.6315	9	580.5106	81.9171
2	95.7062	22.8178	10	700.4457	89.1328
3	119.9845	9.8108	11	781.5985	97.5906
4	145.1224	89.7911	12	903.5728	0.0230
5	291.5586	34.0080	13	1642.7013	126.7168
6	354.3343	394.0165	14	3789.6912	97.7639
7	490.3459	46.6778	15	3878.1455	226.2975
8	542.0271	41.3245			

Table 17. IR vibrational frequencies for Mg^{++} ·2H2O ·1O3d in water solvent background.

Mg-3H₂O-1O₃d-water

	Freq(1/cm)	Inten(KM/Mol)		Freq(1/cm)	Inten(KM/Mol)
1	36.6479	1.7043	18	521.7469	60.1021
2	76.7653	1.9347	19	531.8776	109.1781
3	89.8817	5.4558	20	623.0574	150.4767
4	104.6360	13.0630	21	651.4581	122.9416
5	119.7229	45.9817	22	783.3609	127.5491
6	127.3714	40.6130	23	908.6989	2.5823
7	138.8504	29.6584	24	1097.7404	478.5693
8	182.2291	64.2177	25	1628.3596	145.8792
9	216.8079	45.9305	26	1629.5276	61.2692
10	295.8917	96.1946	27	1638.3958	161.2022
11	311.4384	181.7202	28	2625.5293	1299.8824
12	335.3939	100.0907	29	3792.9644	88.5945
13	348.1166	294.5841	30	3798.9314	75.4685
14	376.2697	304.5839	31	3842.2229	71.6393
15	444.8919	163.1356	32	3880.7100	195.8975
16	470.8790	60.6494	33	3892.1118	185.3123
17	495.6227	32.2330			

Table 18. Energies, geometries, charges and continuous spectra for $Mg^{++} \cdot n(H_2O)$ after geometry optimization.

	Geometry	Frequency
$Mg^{++} \cdot 1H_2O$	 E= -275.7920 a.u.	
$Mg^{++} \cdot 2H_2O$	 E= -352.3408 a.u.	
$Mg^{++} \cdot 3H_2O$	 E= -428.8654 a.u.	 with 1 imaginary frequency -110.04 cm^{-1}
$Mg^{++} \cdot 4H_2O$	Convergence failure	
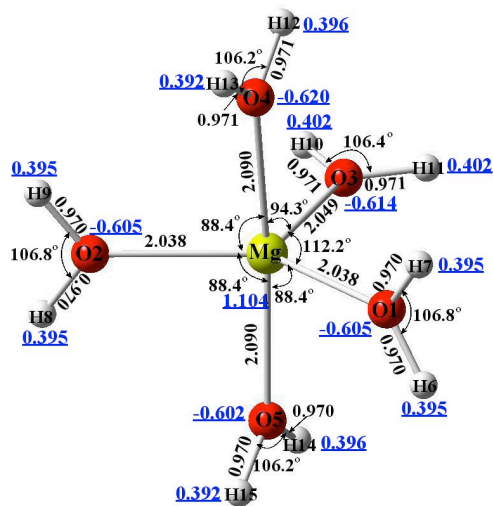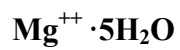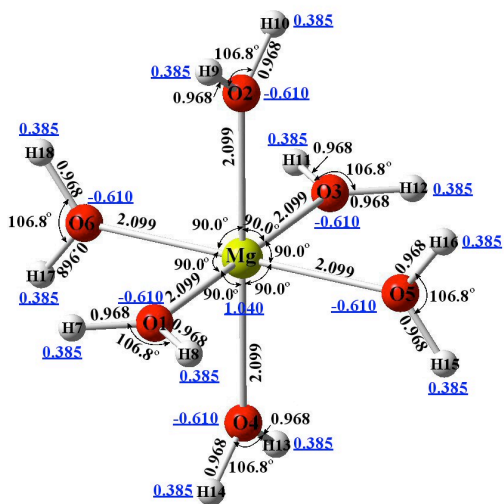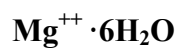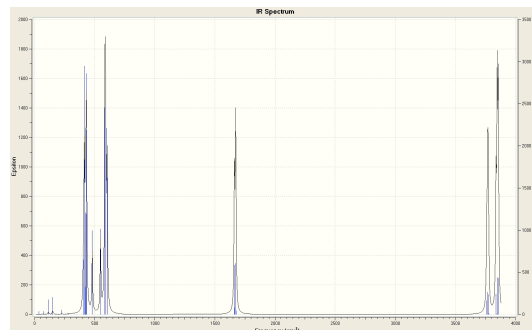
$Mg^{++} \cdot 5H_2O$	 E= -581.8495 a.u.	
$Mg^{++} \cdot 6H_2O$	 E= -658.3220 a.u.	
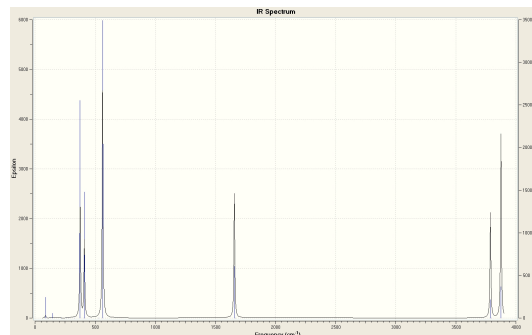
Table 19. IR vibrational frequencies for Mg^{++} and 1, 2 3 H$_2$O.

	Mg2-1H$_2$O		Mg2-2H$_2$O		Mg2-3H$_2$O	
	Freq(1/cm)	Inten(KM/Mol)	Freq(1/cm)	Inten(KM/Mol)	Freq(1/cm)	Inten(KM/Mol)
1	524.9958	397.1609	47.6418	5.8169	-110.0384	0.0000
2	562.7909	56.5400	47.6423	5.8168	92.1857	1.6716
3	707.1497	134.1055	94.2850	0.0000	93.9002	0.1361
4	1679.4133	128.6569	411.2204	0.0000	98.4108	1.1277
5	3626.1953	300.7475	515.7166	361.6000	117.2266	0.0069
6	3676.2710	443.8060	515.7193	361.5994	153.2765	0.0000
7			639.0405	86.8866	389.5321	0.0911
8			679.2854	144.9002	477.7843	0.0000
9			679.2866	144.8996	484.8981	269.6448
10			1681.9615	270.9202	499.6586	654.8561
11			1683.7676	0.0000	527.9147	7.5676
12			3662.9404	533.5046	546.0275	49.3016
13			3669.5151	0.0000	629.2053	157.0193
14			3720.0610	388.6822	642.3626	182.5837
15			3720.0635	388.6820	674.3247	226.7569
16					1681.9235	218.7211
17					1682.8740	171.1304
18					1690.2241	29.0474
19					3705.1223	288.0381
20					3709.6853	354.0846
21					3717.5779	8.0459
22					3767.5979	327.6387
23					3772.1399	126.2290
24					3774.5503	517.6923

Mg++ with 4 H2O has failed to OPT.

Table 20. IR vibrational frequencies for Mg^{++} 5 H_2O.

Mg2-5H₂O

	Freq(1/cm)	Inten(KM/Mol)		Freq(1/cm)	Inten(KM/Mol)
1	36.9772	0.3281	22	479.3806	119.3408
2	76.0194	0.6860	23	548.4352	139.6399
3	93.8325	0.0000	24	562.8165	0.0000
4	113.9833	5.0327	25	585.5466	447.9908
5	131.1920	0.0000	26	591.6745	333.9829
6	139.2785	0.0037	27	603.4382	285.2846
7	147.4520	0.0142	28	1662.5886	244.0411
8	150.9077	7.6384	29	1663.4694	33.5701
9	208.9098	0.0000	30	1672.5835	253.2089
10	226.3208	3.0245	31	1673.8951	116.8317
11	278.4733	0.2736	32	1678.0106	18.4284
12	279.9689	0.5145	33	3761.8977	153.6506
13	344.8745	0.0000	34	3769.7446	248.4844
14	346.2646	0.0359	35	3769.9565	12.8060
15	405.8826	66.0982	36	3775.1189	223.5837
16	409.0751	0.0000	37	3779.8945	11.2348
17	413.5298	305.6091	38	3838.4670	233.9906
18	421.5649	34.3217	39	3848.1477	8.9685
19	423.1540	128.2421	40	3848.7427	421.2361
20	428.4174	127.8762	41	3856.9824	0.0000
21	431.5977	309.3397	42	3857.6836	417.2452

Table 21. IR vibrational frequencies for Mg^{++} 6 H$_2$O.

Mg2-6H$_2$O

	Freq(1/cm)	Inten(KM/Mol)		Freq(1/cm)	Inten(KM/Mol)
1	87.5802	5.3230	27	410.2538	151.9207
2	87.5802	5.3230	28	531.0556	0.0000
3	87.5802	5.3230	29	531.0556	0.0000
4	104.0325	0.0000	30	531.0556	0.0000
5	104.0325	0.0000	31	562.3797	492.2786
6	104.0325	0.0000	32	562.3797	492.2786
7	147.3033	2.0745	33	562.3797	492.2786
8	147.3033	2.0745	34	1657.8409	0.0000
9	147.3033	2.0745	35	1657.8409	0.0000
10	217.5315	0.0000	36	1658.0634	252.4936
11	217.5315	0.0000	37	1658.0634	252.4936
12	261.9888	0.0000	38	1658.0634	252.4936
13	261.9888	0.0000	39	1664.3148	0.0000
14	279.3725	0.0000	40	3786.8391	0.0000
15	279.3725	0.0000	41	3786.8391	0.0000
16	279.3725	0.0000	42	3787.8892	205.9266
17	324.6595	0.0000	43	3787.8892	205.9266
18	374.5719	0.0000	44	3787.8892	205.9266
19	374.5719	0.0000	45	3794.0774	0.0000
20	374.5719	0.0000	46	3875.2148	0.0000
21	375.3512	240.3760	47	3875.2148	0.0000
22	375.3512	240.3760	48	3875.2148	0.0000
23	375.3512	240.3760	49	3875.5796	358.0226
24	406.8894	0.0000	50	3875.5796	358.0226
25	410.2538	151.9207	51	3875.5796	358.0226
26	410.2538	151.9207			